iScience

CellPress
OPEN ACCESS

Article

# Steroidogenic factor 1 protects mice from obesity-induced glucose intolerance via improving glucose-stimulated insulin secretion by beta cells

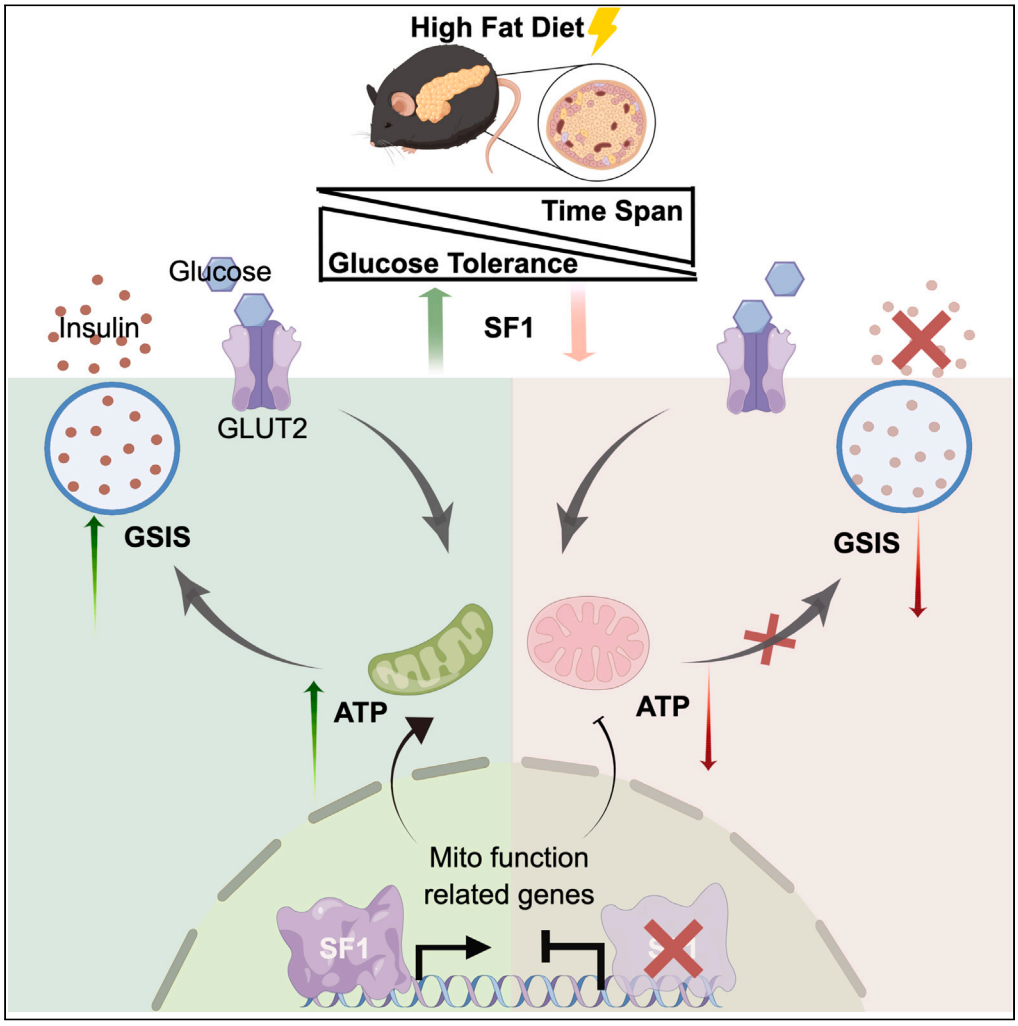


Yan Guo, Liehua Liu, Yanglei Cheng, ..., Hongyu Guan, Haipeng Xiao, Yanbing Li

ghongy@mail.sysu.edu.cn (H.G.)
xiaohp@mail.sysu.edu.cn (H.X.)
liyb@mail.sysu.edu.cn (Y.L.)

## Highlights

Steroidogenic factor 1 (SF1) was highly expressed in beta cells of obese non-diabetic mice and human

SF1 protects against HFD-induced glucose intolerance in mice by improving GSIS

SF1 improves GSIS upon lipotoxicity potentially by promoting mitochondrial functions

Guo et al., iScience 26, 106451
April 21, 2023 
https://doi.org/10.1016/j.isci.2023.106451

iScience

CellPress
OPEN ACCESS

Article

# Steroidogenic factor 1 protects mice from obesity-induced glucose intolerance via improving glucose-stimulated insulin secretion by beta cells

Yan Guo,[1,2] Liehua Liu,[1,2] Yanglei Cheng,[1,2] Hai Li,[1] Xuesi Wan,[1] Jiajing Ma,[1] Juan Liu,[1] Weiwei Liang,[1] Pengyuan Zhang,[1] Jie Chen,[1] Xiaopei Cao,[1] Hongyu Guan,[1,*] Haipeng Xiao,[1,*] and Yanbing Li[1,3,*]

## SUMMARY

**As a potential druggable nuclear receptor, steroidogenic factor 1 (SF1) regulates obesity and insulin resistance in the ventromedial hypothalamic nucleus. Herein, we sought to demonstrate its expression and functions in islets in the development of obesity-induced diabetes. SF1 was barely detected in the beta cells of lean mice but highly expressed in those of non-diabetic obese mice, while decreased in diabetic ones. Conditional deletion of SF1 in beta cells predisposed diet-induced obese (DIO) mice to glucose intolerance by perturbing glucose-stimulated insulin secretion (GSIS). Consistently, forced expression of SF1 restored favorable glucose homeostasis in DIO and *db/db* mice by improving GSIS. In isolated islets and MIN6, overexpression of SF1 also potentiated GSIS, mediated by improvement of mitochondrial ATP production. The underlying mechanisms may involve oxidative phosphorylation and lipid metabolism. Collectively, SF1 in beta cell preserves GSIS to promote beta-cell adaptation to obesity and hence is a potential therapeutic target for obesity-induced diabetes.**

## INTRODUCTION

Type 2 diabetes mellitus (T2DM) results from insulin resistance and ensuing beta-cell deficiency, among which obesity plays a predominant role.[1,2] Obesity-induced diabetes affects more than 400 million people worldwide. At the preliminary stage of obesity-induced diabetes, beta cells experience hyperplasia and enhanced insulin secretion to compensate for insulin resistance in peripheral tissues to maintain glucose homeostasis in obese individuals. Failure of this compensation leads to the development of progressive hyperglycemia.[1,3] Identifying genes involved in beta-cell compensation and decompensation in obesity may shed light on the pathophysiology of T2DM and provide new insights into therapeutic strategies for preserving beta-cell function.

Nuclear receptors (NRs) are critical factors in various physiological and pathophysiological processes. The ligand-dependent activation of NRs has established them as druggable genes with promising therapeutic value for various diseases.[4] Notably, a member of the NR5A family of NRs, namely, steroidogenic factor 1 (SF1, also known as NR5A1), which is highly expressed in steroidogenic organs such as the adrenal gland and gonads, has been also detected in the non-steroidogenic tissues such as ventromedial hypothalamic nucleus (VMH) and found to modulate key metabolic processes.[5] SF1 is essential for organic development and steroidogenesis by activating the genes involved in cholesterol homeostasis.[6] In addition, SF1 promotes adenosine triphosphate (ATP) production by upregulating target genes involved in glycolysis and mitochondrial oxidative phosphorylation (OXPHOS) in the adrenal gland.[7] Interestingly, SF1 deletion causes structural and functional abnormalities in VMH neurons that contribute to thermogenic deficiency, leptin insensitivity, and hyperorexia, thereby contributing to obesity after a high-fat diet (HFD).[8,9] Notably, Liu et al. reported that the Gly146Ala variant of SF1 predisposed Han Chinese subjects to insulin resistance and T2DM,[10] suggesting that SF1 might play a role in glucose homeostasis in addition to its role in obesity in humans. Mazilu et al. reported that ablation of SF1 causes dysplasia of pancreatic islets in zebrafish, implying that SF1 is expressed in islets.[11] Of specific interest are the expression and potential effects of SF1 in islets on the progression of obesity-induced diabetes. The specific molecular mechanisms remain to be clarified.

[1]Department of Endocrinology and Diabetes Center, The First Affiliated Hospital, Sun Yat-sen University, Guangzhou, Guangdong 510080, China

[2]These authors contributed equally

[3]Lead contact

*Correspondence: ghongy@mail.sysu.edu.cn (H.G.), xiaohp@mail.sysu.edu.cn (H.X.), liyb@mail.sysu.edu.cn (Y.L.)

https://doi.org/10.1016/j.isci.2023.106451

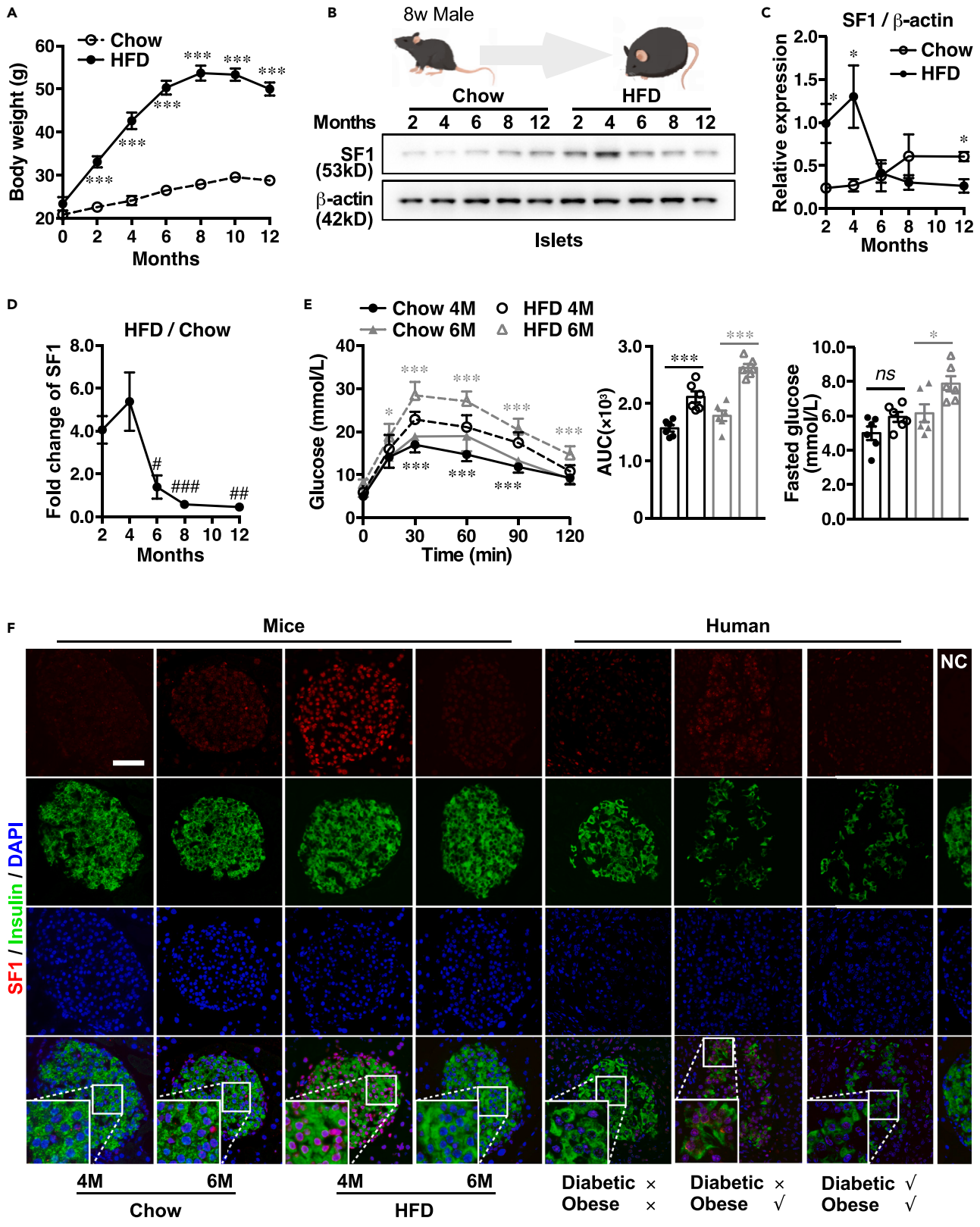
A
Chow
HFD
Body weight (g)
Months
B
8w Male
Chow
HFD
Months
SF1 (53kD)
β-actin (42kD)
Islets
C
SF1 / β-actin
Chow
HFD
Relative expression
Months
D
HFD / Chow
Fold change of SF1
Months
E
Chow 4M
Chow 6M
HFD 4M
HFD 6M
Glucose (mmol/L)
Time (min)
AUC(×10³)
Fasted glucose (mmol/L)
ns
F
Mice
Human
NC
SF1 / Insulin / DAPI
4M
6M
Chow
4M
6M
HFD
Diabetic ×
Obese ×
Diabetic ×
Obese √
Diabetic √
Obese √

**Figure 1. Expression of SF1 in pancreatic beta cells of mice and human**

(A) Body weight of male mice fed by Chow diet or HFD for the indicated time span. Data are expressed as means ± SEM (n = 6).

(B) Representative immunoblots with SF1 (53 kDa) and β-actin (42 kDa) in the islets of male mice fed by Chow diet or HFD for the indicated time span.

(C) Protein levels of SF1 were quantified, normalized to those of β-actin for each sample shown in (B). Data are expressed as mean ± SEM (n = 3).

(D) Fold change of SF1 protein levels in the islets upon HFD relative to those upon Chow diet shown in (B). Data are expressed means ± SEM (n = 3).

(E) GTT and the AUC of male mice fed by Chow diet or HFD for 4 or 6 months (i.p. glucose 1 g/kg). Results are means ± SEM (n = 6).

(F) Representative IF images for SF1 expression in the islets of male mice fed by HFD for 4 or 6 months, and the aged-matched counterparts fed with Chow diet; representative IF images for SF1 expression in the islets of a non-diabetic lean patient, a non-diabetic obese patient, and a diabetic obese patient. Scale bars, 50 μm. NC: negative control using SFI blocking peptide.

For (A) and (E), mice were fasted for 15 h. For (B) and (F), similar images were obtained in 3 additional independent experiments. Significant difference: $^{*}p < 0.05$, $^{***}p < 0.001$, $^{ns}P \geq 0.05$ versus the age-matched control mice; $^{\#}p < 0.05$, $^{\#\#}p < 0.01$, $^{\#\#\#}p < 0.001$ versus the mice fed with an HFD for 4 months. See also Figures S1 and S2.

Herein, we sought to 1) examine the temporal changes in beta-cell SF1 gene expression in models of beta-cell compensation and failure; 2) determine its mode of action in beta-cell functions and glucose homeostasis upon dietary manipulation; and 3) further delineate the underlying mechanisms.

## RESULTS

### Steroidogenic factor 1 is upregulated with the beta-cell compensation but is downregulated with the decompensation for obesity

To detect SF1 expression in islets in the pathogenesis of obesity, we fed 8-week-old C57BL/6J male mice an HFD to generate a diet-induced obesity (DIO) model (Figure 1A). Immunoblotting was performed to analyze SF1 expression in the islets isolated from DIO mice and the age-matched counterparts at the indicated time points (Figure 1B). As depicted in Figure 1B, C, and D, SF1 was barely detected in the islets of lean mice but highly expressed in those of mice fed an HFD in the short term (specifically within 4 months). However, SF1 in the islets tended to decrease upon long-term HFD consumption (more than 6 months). As shown in Figure 1E, the mice fed with HFD for 4 months presented impaired glucose tolerance but normal fasted blood glucose, which implied that beta cells were in the compensated stage. However, those fed an HFD for 6 months suffered not only more severe glucose intolerance but also impaired fasted glucose compared with the age-matched Chow mice, which indicated beta-cell decompensation. Immunofluorescence (IF) experiments were also performed to detect SF1 expression (Figure 1F). Congruously, SF1 staining was robustly upregulated in the beta cells of mice upon four-month HFD feeding compared with that of the control lean mice, while expression of SF1 in the beta cells of mice upon long-term HFD declined to the comparable level as that of the age-matched Chow mice (Figure 1F). We also involved genetic obese/diabetic mouse model to analyze SF1 expression. As shown in Figure S1A, body weight of both *ob/ob* and *db/db* mice were significantly higher than that of the control group. However, there were no statistically significant differences in fasted/refed glucose between *ob/ob* mice and the control mice (Figure S1B), since hyperglycemia tends to remit due to compensatory hyperinsulinemia at the age of 12 weeks, as reported before.[12] While *db/db* mice, in which beta cells failed to compensate for obesity, represented obvious hyperglycemia compared with the lean control (Figure S1C). Interestingly, SF1 was conformably highly expressed in the beta cells of *ob/ob* mice but hardly detected in those of *db/db* mice (Figure S1D). In order to further confirmed SF1 expression in the islets of mice, we used testis slides as positive control (Figure S2A), as well as *in situ* hybridization (RNAscope) detecting SF1 mRNA shown in Figure S2B. With regard to human, SF1 was highly expressed in the beta cells of non-diabetic obese patient, compared with that of the non-diabetic non-obese patient and the diabetic obese patient (Figure 1F). The high expression of SF1 was also confirmed by RNAscope (Figure S2C). Collectively, SF1 expression was associated with beta-cell functions during the adaptive compensation to obesity-induced insulin resistance. Whether the expression of SF1 protects beta cells from obesity-induced failure remains to be studied.

### Establishment of conditional beta-cell steroidogenic factor 1 knockout mice

To determine the functions of SF1 in the beta cells of obese adult mice, we generated an inducible, beta-cell specific, heterozygous/homozygous SF1-knockout mouse model and control littermates on a C57BL/6J background. These mice were injected daily with tamoxifen (TAM) for 10 days to generate $\beta SF1^{+/+}$, $\beta SF1^{+/-}$, and $\beta SF1^{-/-}$ mice (Figure 2A). Ten days of TAM administration had no obvious impact on body weight or glucose tolerance on Chow diet (Figures S3A and S3B). Knockout of SF1 in beta cells was verified by genomic DNA detection, immunoblotting, and IF (Figure 2B). As observed in Figure 2C, the PCR products were successfully cloned using primers that targeted the upward and downward directions of floxed SF1 respectively, in the islets of $\beta SF1^{-/-}$ mice of both sexes. SF1 ablation in the islets but not in

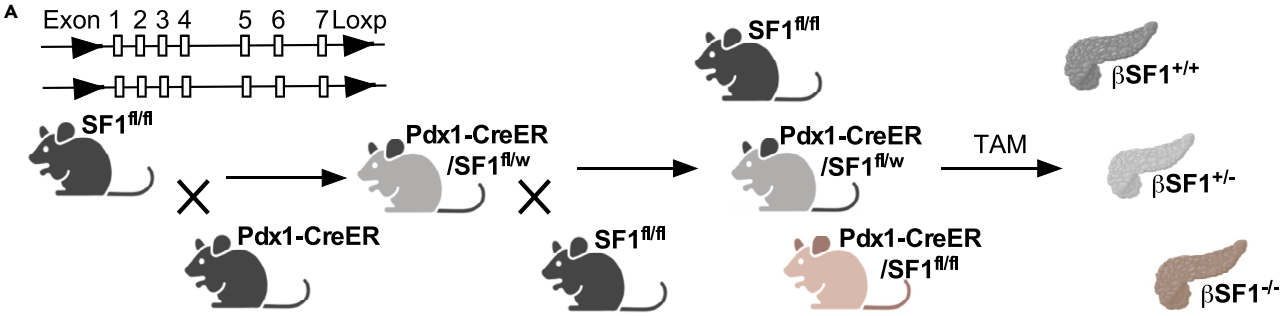
A
Exon 1 2 3 4 5 6 7Loxp
SF1fl/fl
Pdx1-CreER
Pdx1-CreER /SF1fl/w
SF1fl/fl
Pdx1-CreER /SF1fl/w
TAM
βSF1+/+
βSF1+/-
Pdx1-CreER
SF1fl/fl
Pdx1-CreER /SF1fl/fl
βSF1-/-

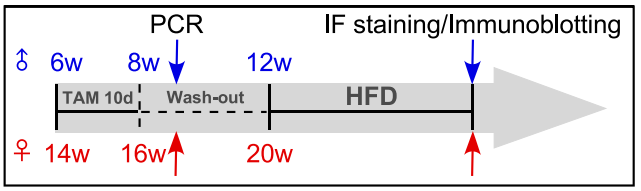
B
PCR
IF staining/Immunoblotting
♂ 6w 8w 12w
TAM 10d
Wash-out
HFD
♀ 14w 16w 20w

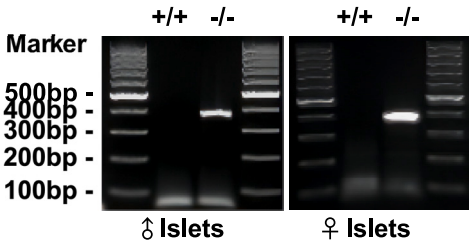
C
+/+ -/- +/+ -/-
Marker
500bp -
400bp -
300bp -
200bp -
100bp -
♂Islets
♀Islets

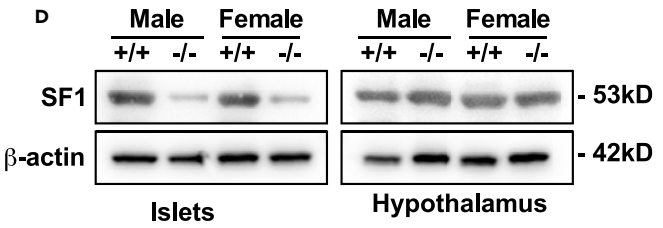
D
Male Female Male Female
+/+ -/- +/+ -/- +/+ -/- +/+ -/-
SF1
β-actin
- 53kD
- 42kD
Islets
Hypothalamus

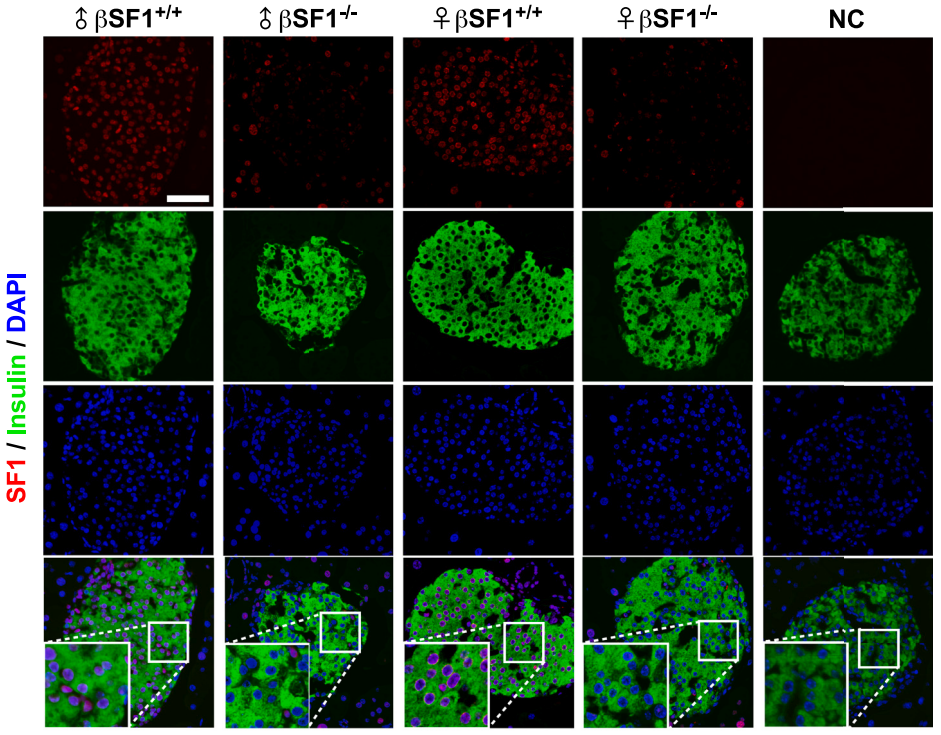
E
♂βSF1+/+
♂βSF1-/-
♀βSF1+/+
♀βSF1-/-
NC
SF1 / Insulin / DAPI

**Figure 2. Conditional knockout (CKO) of SF1 in pancreatic beta cells**

(A) Generation of homozygous CKO mice (βSF1$^{-/-}$), the control littermates (βSF1$^{+/+}$) and the heterozygous mice (βSF1$^{+/-}$) in C57BL/6J background.

(B) Experimental design to assess SF1 knockout in islets.

(C) Ablation of SF1 was confirmed by PCR using the total DNA of islets (βSF1$^{+/+}$ and βSF1$^{-/-}$). Similar images were obtained in 3 additional independent experiments.

(D) Expression of SF1 in the islets and the hypothalamus from HFD mice was detected by immunoblotting. β-actin served as control. Similar images were obtained in 3 independent experiments.

(E) Representative IF images for SF1 staining in pancreatic islets of βSF1$^{+/+}$ and βSF1$^{-/-}$ mice (male and female) fed with HFD. Scale bars, 50 μm. NC: negative control using SFI blocking peptide. Similar images were obtained in 3 independent experiments.

For (C), βSF1$^{+/+}$ and βSF1$^{-/-}$ mice without being fed with HFD were sacrificed for analysis. For (D) and (E), βSF1$^{+/+}$ and βSF1$^{-/-}$ mice were sacrificed for analysis after HFD feeding. See also Figure S3.

the hypothalamus of βSF1$^{-/-}$ male/female DIO mice, was confirmed by immunoblotting (Figure 2D). IF was also conducted to confirm that SF1 was specifically deleted in the beta cells of βSF1$^{-/-}$ mice (Figure 2E).

## Conditional knockout of steroidogenic factor 1 in pancreatic beta cells accelerates glucose intolerance and impaired fasting glucose in both male and female diet-induced obese mice

Male mice aged 6–12 weeks are commonly used as DIO models, while female mice are less susceptible to diet-induced metabolic impairments unless they are aged.[13,14] As shown in Figure 3A, after a baseline intraperitoneal (i.p.) glucose tolerance test (GTT), both females and males of different genotypes (βSF1$^{+/+}$, βSF1$^{+/-}$, and βSF1$^{-/-}$) were subjected to an HFD regimen, and subsequent GTT was performed monthly. At baseline before dietary induction, there were no differences in glucose intolerance or fasted glucose among the βSF1$^{+/+}$, βSF1$^{+/-}$, and βSF1$^{-/-}$ groups of both females and males (Figure 3B). It was not until the eighth week since HFD administration for the males and the twelfth week for the females that the difference of glucose tolerance among groups of different genotypes became significant (Figure 3C). Male and female βSF1$^{-/-}$ mice but not βSF1$^{+/-}$mice exhibited higher blood glucose excursion at each time point and a larger area under the curve (AUC) of blood glucose after an i. p. glucose challenge than their βSF1$^{+/+}$ counterparts, after HFD feeding (Figure 3C). As shown in Figure 3D, insulin sensitivity measured by the area over the curve (AOC) in the insulin tolerance test (ITT) was similar among the three groups, although body weight in the βSF1$^{-/-}$ group was higher than that in the βSF1$^{+/+}$ and βSF1$^{+/-}$ groups (Figure 3E). Thus, the glucose metabolic exacerbation accompanying beta-cell SF1 knockout was not caused by insulin resistance. As depicted in Figure 3F, βSF1$^{-/-}$ mice failed to raise insulin levels comparable to those of their control littermates in response to glucose challenge. Notably, male βSF1$^{-/-}$ mice exhibited higher fasted glucose after 8 weeks of HFD feeding, whereas it was not until 12 weeks later that the difference between female βSF1$^{-/-}$ and βSF1$^{+/+}$ mice became significant (Figure 3G). And the AUC of fasted glucose in male βSF1$^{-/-}$ mice was significantly larger than that in the βSF1$^{+/+}$ mice (Figure 3G). Instead, the AUC among different groups of female mice represented no significant statistic difference (Figure 3G). As shown in Figure S4A, no obvious difference in cell composition or islet morphology between the βSF1$^{+/+}$ and βSF1$^{-/-}$ groups were revealed by histological analysis. These results suggested that SF1 ablation predisposed beta cells to insulin secretion deficiency and abnormal glucose metabolism upon HFD consumption rather than a Chow diet. Intriguingly, male mice were more susceptible than female to the phenotypes caused by SF1 knockout.

## Adeno-associated virus–mediated steroidogenic factor 1 overexpression in beta cells improves GSIS in diabetic mice

As mentioned in Figures 1 and S1D, SF1 was hardly detected in the islets of either diet-induced or hereditary diabetic mice. To further evaluate the effects of SF1 on the islets of diabetic mice, AAV8-Ins1-SF1 and AAV8-Ins1-Vector were, respectively delivered into mice fed an HFD for 6 months and 12-week-old *db/db* mice via intraperitoneal injection, after which metabolic experiments were conducted at the indicated time points (Figure 4A). Overexpression of SF1 in beta cells but not in other tissues of DIO mice was determined by immunoblotting (Figure S5A) and IF (Figure S5B). Intriguingly, as early as 4 days after adeno-associated virus (AAV) injection, overexpression of SF1 in beta cells of DIO mice increased the instant insulin response to an i.p. glucose load within 10 min (Figure 4B). Similarly, insulin secretion was significantly recovered in one week after AAV8-Ins1-SF1 transfection in *db/db* mice (Figure 4B). As expected, SF1 restoration significantly ameliorated glucose intolerance in both DIO and *db/db* mice, as analyzed by GTT (Figure 4C). Notably, reversal of hyperglycemia was observed in both DIO and *db/db* mice after the reintroduction of beta-cell SF1. Serum glucose levels of AAV8-Ins1-SF1 mice in the refed state were significantly lower than those of AAV8-Ins1-Vector mice from the first week after AAV injection to the end of observation

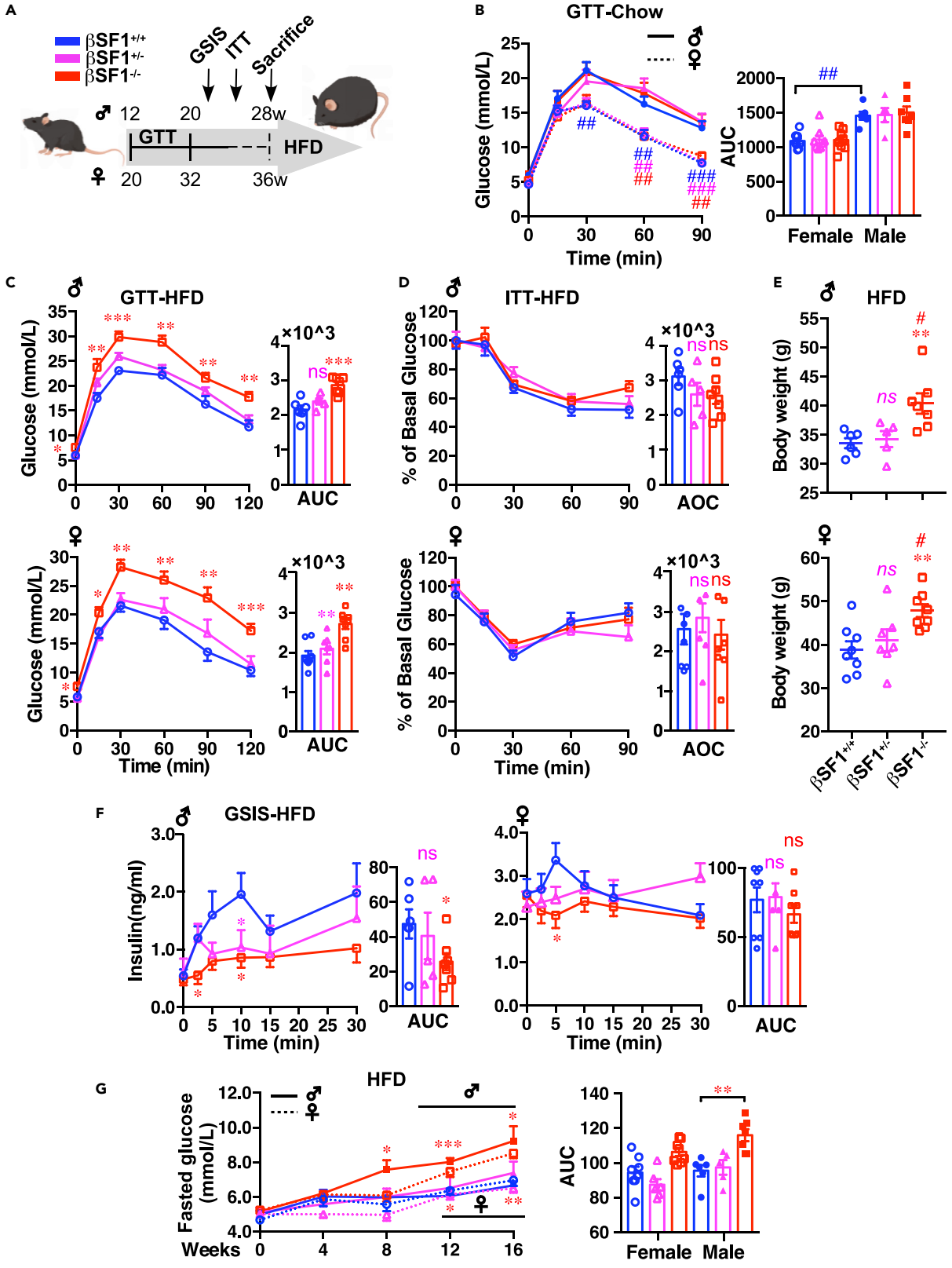
A
βSF1+/+
βSF1+/-
βSF1-/-
GSIS
ITT
Sacrifice
♂ 12
20
28w
GTT
HFD
♀ 20
32
36w
B
GTT-Chow
Glucose (mmol/L)
Time (min)
AUC
Female
Male
C
GTT-HFD
Glucose (mmol/L)
Time (min)
AUC
D
ITT-HFD
% of Basal Glucose
AOC
E
HFD
Body weight (g)
βSF1+/+
βSF1+/-
βSF1-/-
F
GSIS-HFD
Insulin(ng/ml)
Time (min)
AUC
G
HFD
Fasted glucose (mmol/L)
Weeks
AUC
Female
Male

**Figure 3. Depletion of SF1 in beta cells impairs glycometabolism parameters in DIO male/female mice**

(A) Experimental design to assess the impact of beta-cell SF1 deletion on male/female mice fed with HFD. 12-week-old male and 20-week-old female mice were used.

(B) Baseline GTT and the AUC results of Chow-fed mice of different genotypes (i.p. 2.0 g/kg glucose). $^{\#}p < 0.05$, $^{\#\#}p < 0.01$, $^{\#\#\#}p < 0.001$, versus male mice.

(C) GTT and the AUC results of HFD-fed mice of different genotypes (i.p. 2.0 g/kg glucose).

(D) ITT and the area over curve (AOC) results of HFD-fed mice of different genotypes (Fasted for 5 h, i.p. 0.75 U/kg).

(E) Body weight of HFD-fed mice of different genotypes.

(F) Glucose stimulated insulin secretion (GSIS) and the AUC results of HFD-fed mice. (i.p. 3.0 g/kg glucose).

(G) Fasted blood glucose and the AUC from 0 to 16 weeks after HFD feeding.

For the metabolic experiments in (B)-(G), the mice were fasted for 15 h unless otherwise indicated. The graphics represent the means ± SEM [$\beta SF1^{+/+}$ (male, n = 6; female, n = 8), $\beta SF1^{+/-}$ (male, n = 5; female, n = 7) and $\beta SF1^{-/-}$ (male, n = 7; female, n = 8)]. For (C)-(F), male mice were fed an HFD for 8 weeks, female for 12 weeks; Significant difference: $^{*}p < 0.05$, $^{**}p < 0.01$, $^{***}p < 0.001$, $^{ns}P \geq 0.05$ versus the $\beta SF1^{+/+}$ group; $^{\#}p < 0.05$ versus the $\beta SF1^{+/-}$ group. See also Figure S4.

(Figure 4D). In addition, fasted glucose was markedly reduced in the SF1 group beginning at 8 weeks after AAV8 delivery (Figure 4D). However, overexpression of SF1 in beta cells did not result in any significant change in insulin sensitivity in either DIO or *db/db* mice, despite a decrease in body weight in AAV8-Ins1-SF1 DIO mice (Figures 4E and 4F). Taken together, the reexpression of beta-cell SF1 relieved both fasted and postchallenged blood glucose in diabetic mice, probably due to improving beta-cell functions.

## Steroidogenic factor 1 potentiates GSIS in beta cells by restoring ATP production

Based on the finding that SF1 deficiency impaired GSIS in mice upon HFD feeding but not Chow feeding, it is rational to assume that SF1 protected beta cells from lipotoxicity. To further investigate how SF1 exerts insulinotropic effects, pancreatic islets were isolated from $\beta SF1^{-/-}$ and $\beta SF1^{+/+}$ DIO mice, kept in palmitate (Palmitate Acid (PA), 0.4 mM) and pretreated with or without the SF1 agonist 8-Br-cAMP for 48 h before the *in vitro* insulin secretion experiments. As shown in Figure 5A, subsequent GSIS *in vitro* demonstrated that $\beta SF1^{+/+}$ islets responded better to high glucose, which was further provoked by the agonist 8-Br-cAMP pretreatment. $\beta SF1^{-/-}$ islets displayed significantly blunted insulin secretion at high glucose (16.7 mM), which could not be restored by the agonist. Moreover, KCl (30 mM)-stimulated insulin secretion (KSIS) was comparable between these two genotypes (Figure 5B). These results suggested that the effects of SF1 exerted on GSIS were independent of direct closure of $K_{ATP}$ channels and membrane depolarization. We next assessed the impact of SF1 on ATP production. High glucose-stimulated ATP production in $\beta SF1^{-/-}$ islets was decreased by over 50% compared with the control and was not responsive to the agonist (Figure 5C).

To prove that this impaired secretory response was attributed to SF1 deficiency per se, we transfected the islets isolated from male DIO $\beta SF1^{-/-}$ mice with adenovirus expressing SF1 (Ad-GFP-SF1) and control (Ad-GFP-Vector). The transfection efficiency was confirmed by GFP signaling under a fluorescence microscope (Figure 5D). Impaired GSIS in $\beta SF1^{-/-}$ islet cells was noticeably reversed by SF1 re-expression, which was intensified by the agonist (Figure 5E). Consistently, high glucose-induced ATP production was also regained by SF1 under treatment with the agonist (Figure 5F). These data indicated that GSIS restoration by SF1 ectopic expression in $\beta SF1^{-/-}$ islets under lipotoxic stress may be mediated by improved glucose catabolism. GSIS in beta cells involves glucose intake, glycolysis, and oxidative phosphorylation, which lead to ATP synthesis.[15] Given that ATP synthesis during oxidative metabolism in mitochondria is prone to be perturbed by lipotoxicity,[16] we next examined whether SF1 recovered mitochondrial functions through oxygen consumption rate (OCR) analysis. As represented in Figure 5G, SF1 overexpression resulted in higher glucose-stimulated and maximal OCR in $\beta SF1^{-/-}$ islets.

To confirm the above observations, we established insulinoma cell line MIN6 that overexpresses SF1 with a FLAG tag, as determined by immunoblotting (Figure 5H). Analogously, SF1 overexpression boosted basal, glucose-stimulated, and maximal OCR in MIN6 cells, which were further improved by the agonist (Figure 5I). As shown in Figure 5J, SF1 did not alter the $Ca^{2+}$ influx stimulated by KCl (30 mM). Here, we demonstrated that ATP production by mitochondria, instead of calcium or potassium channels, might mediate the favorable effects of SF1 on GSIS in lipotoxicity-challenged beta cells.

## The underlying mechanisms involved in the favorable effects of steroidogenic factor 1 on beta cells identified by bioinformatics analysis

To decipher potential targets of SF1, we conducted RNA-Seq using $\beta SF1^{-/-}$ islets isolated from HFD-fed male mice (n = 3) and transfected with Ad-GFP-Vector/SF1. There were 377 upregulated genes and 58

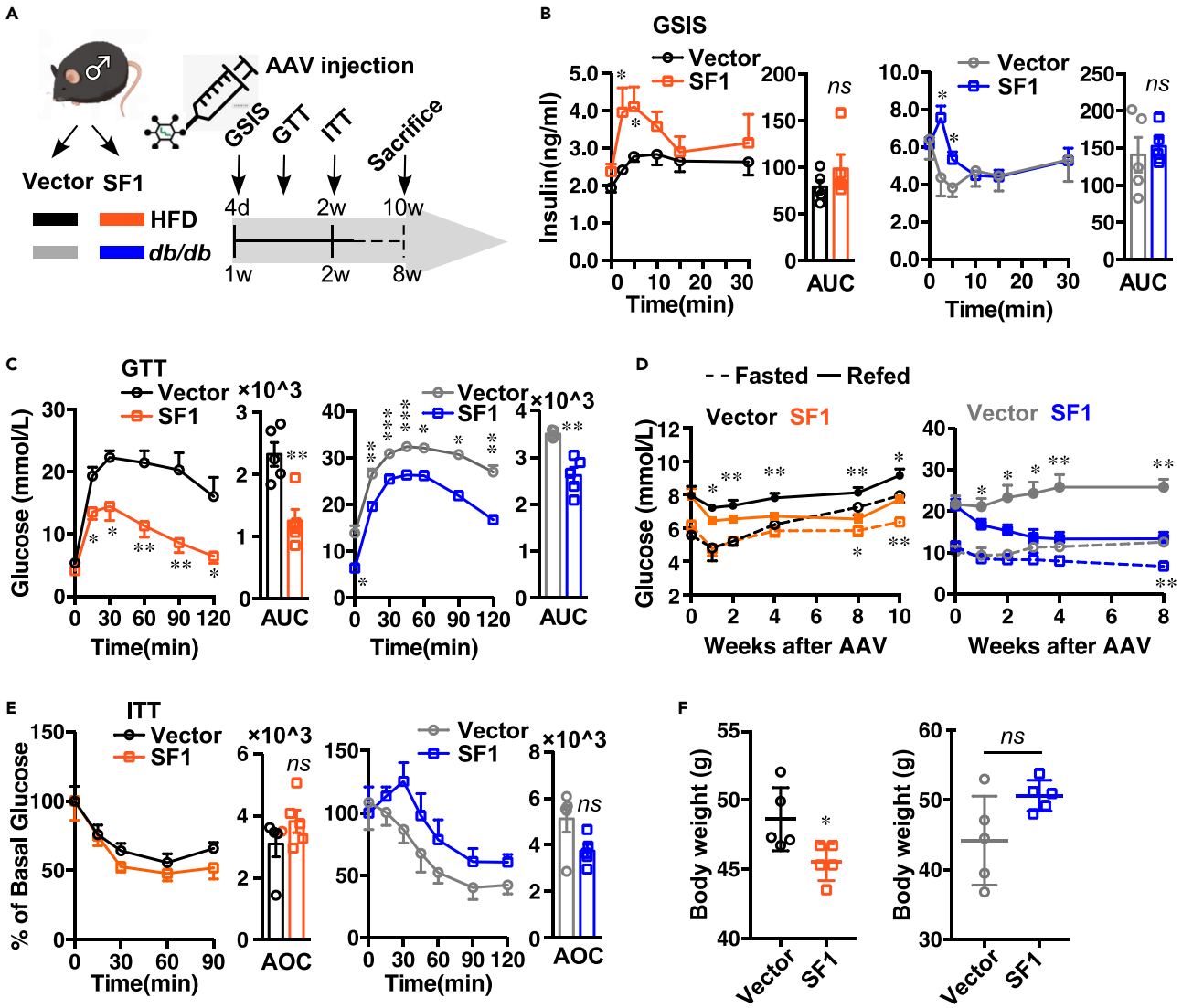


**Figure 4. AAV-mediated beta cell-specific overexpression of SF1 improves glucose homeostasis in diabetic obese mice**

(A) Experimental design to analyze the effects of SF1 over-expressed specifically in beta cells through injection with AAV8-Ins1-SF1 in HFD-fed male mice (HFD for 6 months) and *db/db* mice (12 weeks old). Age-matched mice injected with AAV8-Ins1-Vector served as control.

(B) GSIS and the AUC results of HFD-fed and *db/db* mice injection with AAV8-Ins1-Vector and AAV8-Ins1-SF1 (n = 5, i.p. glucose 3.0 g/kg for HFD-fed mice, 1.5 g/kg for *db/db* mice).

(C) GTT and the AUC results of HFD-fed and *db/db* mice injection with AAV8-Ins1-Vector and AAV8-Ins1-SF1 (n = 5, i.p. glucose 1.0 g/kg).

(D) Fasted and refed (5 h) blood glucose of HFD-fed and *db/db* mice injection with AAV8-Ins1-Vector and AAV8-Ins1-SF1 in different time periods (n = 5).

(E) ITT and the AOC results of HFD-fed and *db/db* mice injection with AAV8-Ins1-Vector and AAV8-Ins1-SF1 (Fasted for 5 h, i.p. insulin 1=.0 U/kg for HFD-fed mice; fasted for 17 h, i.p. insulin 2.0 U/kg for *db/db* mice). n = 5 per group.

(F) Body weight of HFD-fed and *db/db* mice injection with AAV8-Ins1-Vector and AAV8-Ins1-SF1 (n = 5).

For metabolic experiments, DIO mice were fasted for 15 h, while *db/db* mice for 17 h unless otherwise indicated. Values are means ± SEM in each group. Significant difference: *p < 0.05, **p < 0.01, ***p < 0.01, $^{ns}$P ≥ 0.05 versus the AAV8-Ins1-Vector group. See also Figure S5.

downregulated genes in Ad-SF1 islets (Figure 6A). As depicted in the annotations of the Gene Ontology (GO) analysis in Figure 6B, SF1 appeared to be robustly correlated with processes such as lipid metabolic processes, aldehyde dehydrogenase (NAD) activity, and mitochondrial cristae. We also performed gene set enrichment analysis (GSEA) using SF1-related RNA-Seq data. The functions of these core enrichment genes were critical for mitochondrial functions such as oxidative phosphorylation and the electron transport chain (Figure 6C), lipolysis (Figure 6D), and detoxication (Figure 6E). In addition, transcriptional profiling using MIN6-Vector/SF1 was also performed. Kyoto Encyclopedia of Genes and Genomes

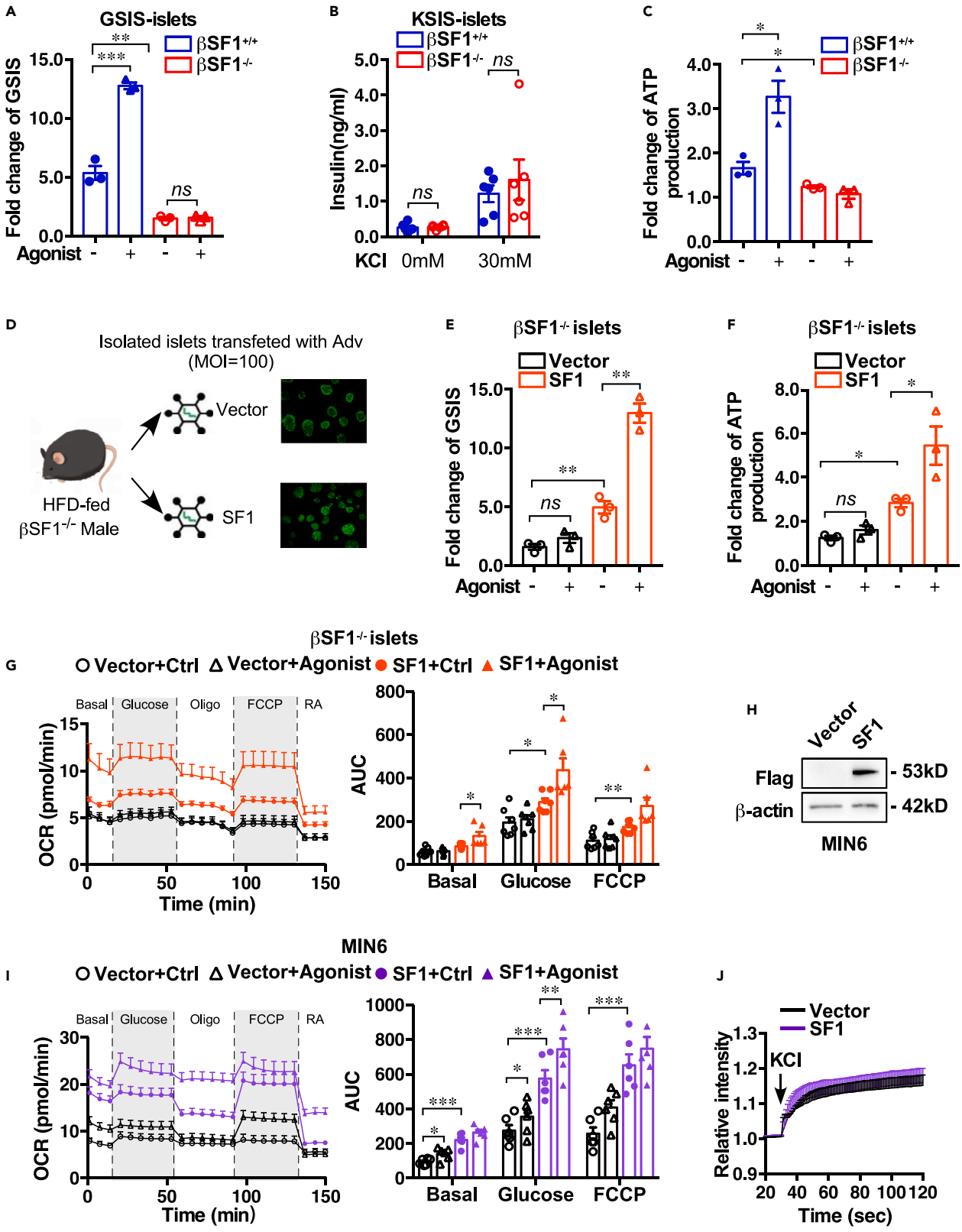
A
GSIS-islets
βSF1+/+
βSF1-/-
Fold change of GSIS
Agonist
B
KSIS-islets
Insulin(ng/ml)
KCl 0mM 30mM
C
Fold change of ATP production
D
Isolated islets transfeted with Adv (MOI=100)
Vector
SF1
HFD-fed βSF1-/- Male
E
βSF1-/- islets
F
βSF1-/- islets
G
βSF1-/- islets
Vector+Ctrl Vector+Agonist SF1+Ctrl SF1+Agonist
Basal Glucose Oligo FCCP RA
OCR (pmol/min)
Time (min)
AUC
H
Flag
β-actin
53kD
42kD
MIN6
I
MIN6
J
Relative intensity
KCl
Time (sec)

**Figure 5. SF1 restoration blunts lipotoxic effects on GSIS in beta cells by alleviating mitochondrial defect**

(A) GSIS of islets from βSF1$^{+/+}$ and βSF1$^{-/-}$ HFD-fed mice, upon basal (3.3 mM) or high (16.7 mM) glucose conditions (n = 3 per group). Islets kept in PA (0.4 mM) were pretreated with or without agonist (8-Br-cAMP 1.0 mM) for 48 h before GSIS assays.

(B) KSIS of islets from βSF1$^{+/+}$ and βSF1$^{-/-}$ HFD-fed mice (n = 6 per group), upon basal (0 mM) or high (30 mM) KCl conditions (containing 3.3 mM glucose). Islets were kept in PA (0.4 mM) before the assay.

(C) ATP production of islets from βSF1$^{+/+}$ and βSF1$^{-/-}$ HFD-fed mice, upon basal (3.3 mM) or high (16.7 mM) glucose conditions (n = 3 per group). Islets kept in PA (0.4 mM) were pretreated with or without agonist (8-Br-cAMP 1.0 mM) for 48 h before ATP assays.

(D) Experimental design to analyze the effects of beta-cell SF1 overexpression on islets upon PA treatment through infection with adenovirus (Adv) encoding GFP-tagged SF1 (Ad-GFP-SF1) at an MOI of 100 for 24 h. Islets in the control groups were infected with the same amount of Ad-GFP-Vector.

(E–G) GSIS (n = 3) (E), ATP production (n = 3) (F), OCR (n = 6) measured by an XF24 respirometer and quantification of AUC (G) of islets from βSF1$^{-/-}$ HFD-fed mice transected with Ad-GFP-Vector and Ad-GFP-SF1 respectively, upon basal (3.3 mM) or high (16.7 mM) glucose conditions. Islets kept in PA (0.4 mM) were pretreated with or without agonist (8-Br-cAMP 1.0 mM) for 48 h before assays.

(H) Representative immunoblots with Flag (SF1, 53 kDa) in MIN6-Vector/SF1. β-actin served as a control.

(I) OCR curve and the AUC of MIN6-Vector/SF1. Cultured cells kept in PA (0.4 mM) were pretreated with or without agonist (8-Br-cAMP 1.0 mM) for 48 h before assays.

(J) Xhrod-1 AM fluorescent intensity of MIN6-Vector/SF1 with 30 mM KCl stimulation (n = 4). MIN6 was kept in PA (0.4 mM) before the assay.

For (A–G), islets were isolated from male mice fed with an HFD for 8 weeks and kept in PA (0.4 mM) before assays. Results are represented as mean ± SEM (Data were calculated using 3 repeats of results for each mouse). Significant difference: *$p < 0.05$, **$p < 0.01$, ***$p < 0.001$ and $^{ns}P \geq 0.05$ vs corresponding control group.

(KEGG) pathway enrichment analysis showed the correlation of SF1 with insulin secretion, the oxytocin signaling pathway, and the mitogen-activated protein kinase (MAPK) pathway cascade (Figure 6F). These analyses further supported that SF1 was associated with energetic metabolism processes such as mitochondrial functions, insulin secretion, and lipid metabolism upon HFD consumption.

## DISCUSSION

In the current research, we have uncovered a novel role of SF1 in beta cells as a facilitator of GSIS in the compensatory adaptation toward obesity-induced diabetes beyond its conventional role as a steroidogenic regulator. These conclusions are supported by the findings that 1) SF1 is highly expressed in the beta cells of non-diabetic obese mice; 2) beta-cell SF1 in obese mice is upregulated with beta-cell compensation for obesity but is decreased with decompensation; 3) beta-cell SF1 deficiency predisposes male/female mice to glucose intolerance and high fasted glucose upon HFD consumption, ensuing from compromised GSIS; 4) restoration of SF1 in beta cells sustainably mitigates glucose intolerance and fasted hyperglycemia by improving GSIS in both dietary and genetic obese-diabetic mice; and 5) SF1 potentiates GSIS by enhancing mitochondrial ATP production. These cumulative findings strongly support the implication of SF1 in the positive regulation of beta-cell functions.

As a steroidogenic factor, SF1 is highly expressed in the adrenal gland and gonad.[5] Recently, an increasing number of studies have found its expression in the non-steroidogenic tissues such as the VMH and identified its vital role in energy metabolism.[17,18] It was reported that SF1 ablation leads to dysplasia of pancreatic islets in zebrafish.[11] An interesting study reported that another member of the NR5A family, NR5A2/LRH1, is involved in neonatal beta cell mass establishment by regulating cell replication and plays a key role in protecting mouse islets against stress-induced apoptosis.[19] Nonetheless, it had not been reported before whether SF1 is expressed in beta cells, especially those of mammals. To our surprise, SF1 was barely detected in the beta cells of lean mice but was highly expressed in those fed an HFD while reduced after long-term HFD consumption when glucose tolerance and fasted glucose were impaired. We demonstrated that SF1 expression correlated with beta-cell adaptation to obesity. Our data provide the first evidence that SF1 was expressed by beta cells in a particular situation and mediates beta-cell compensation for obesity.

Impaired GSIS is a hallmark of obesity-induced beta-cell deficiency. On the one hand, GSIS involves glucose catabolism and mitochondrial ATP production, which blocks $K_{ATP}$ channels and $Ca^{2+}$ influx, finally triggering insulin secretion.[16,20] On the other hand, amplification pathways involving lipid metabolism are thought to be important for GSIS, such as the ATP citrate lyase (ACL)/acetyl-CoA carboxylase (ACC)/malonyl-CoA/carnitine palmitoyltransferase-1 (CPT-1) axis, the glycerolipid/non-esterified fatty acid (NEFA) cycle, and nicotinamide adenine dinucleotide plus hydrogen (NADPH).[21] Electrons are transferred from tricarboxylic acid (TCA) cycle intermediates to the respiratory chain via NADPH across the inner membrane for OXPHOS, which produces ATP.[22] Lipolysis promotes NEFA formation and release from beta cells, which also ameliorates beta-cell lipotoxicity.[21,23] Unfortunately, the existing insulin secretagogues have little positive effect on beta-cell protection by ameliorating either mitochondrial functions or lipid metabolism.[24] It

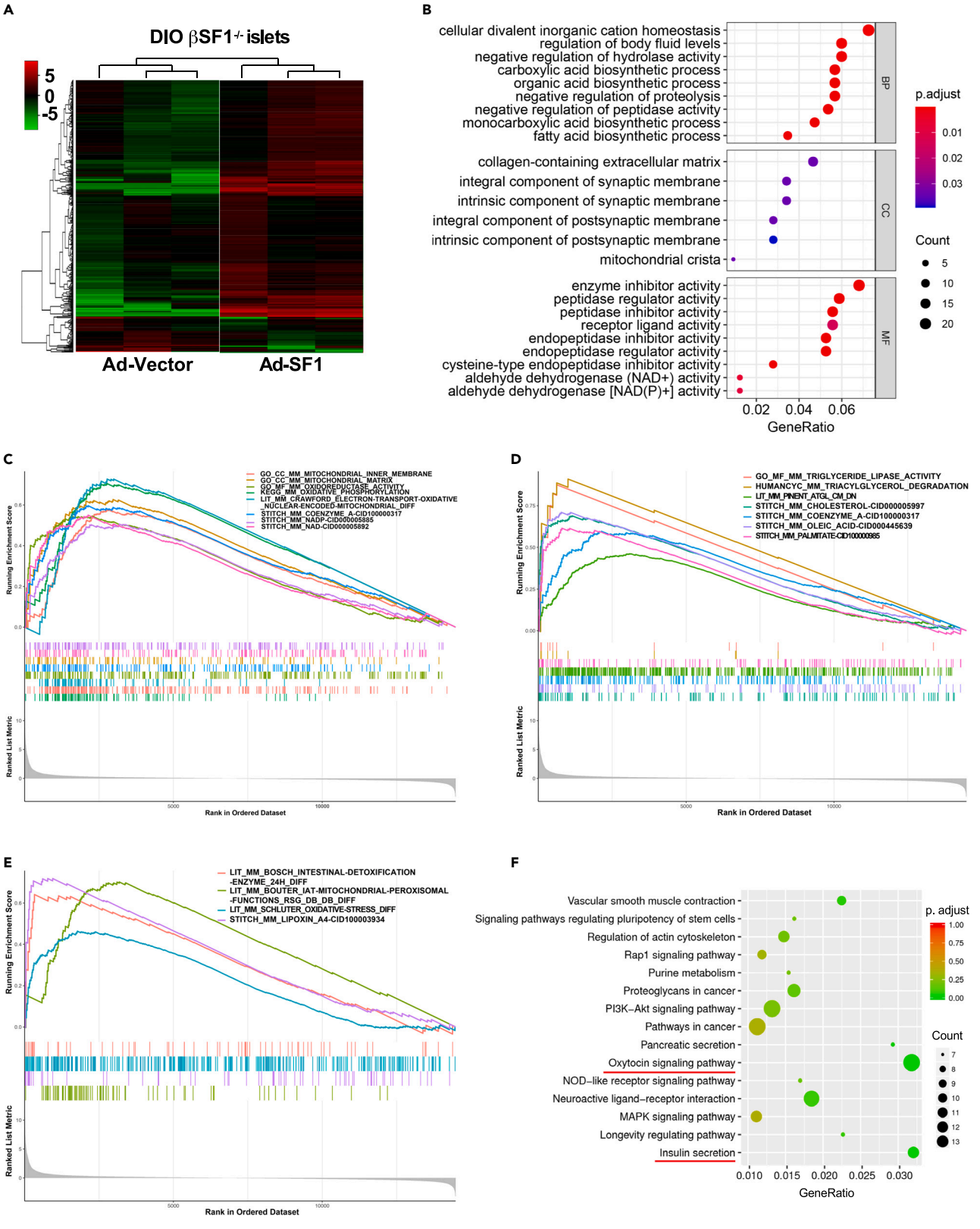
A
DIO βSF1-/- islets
5
0
-5
Ad-Vector
Ad-SF1
B
cellular divalent inorganic cation homeostasis
regulation of body fluid levels
negative regulation of hydrolase activity
carboxylic acid biosynthetic process
organic acid biosynthetic process
negative regulation of proteolysis
negative regulation of peptidase activity
monocarboxylic acid biosynthetic process
fatty acid biosynthetic process
collagen-containing extracellular matrix
integral component of synaptic membrane
intrinsic component of synaptic membrane
integral component of postsynaptic membrane
intrinsic component of postsynaptic membrane
mitochondrial crista
enzyme inhibitor activity
peptidase regulator activity
peptidase inhibitor activity
receptor ligand activity
endopeptidase inhibitor activity
endopeptidase regulator activity
cysteine-type endopeptidase inhibitor activity
aldehyde dehydrogenase (NAD+) activity
aldehyde dehydrogenase [NAD(P)+] activity
BP
CC
MF
p.adjust
0.01
0.02
0.03
Count
5
10
15
20
0.02 0.04 0.06
GeneRatio
C
GO_CC_MM_MITOCHONDRIAL_INNER_MEMBRANE
GO_CC_MM_MITOCHONDRIAL_MATRIX
GO_MF_MM_OXIDOREDUCTASE_ACTIVITY
KEGG_MM_OXIDATIVE_PHOSPHORYLATION
LIT_MM_CRAWFORD_ELECTRON-TRANSPORT-OXIDATIVE_NUCLEAR-ENCODED-MITOCHONDRIAL_DIFF
STITCH_MM_COENZYME_A-CID100000317
STITCH_MM_NADP-CID000005885
STITCH_MM_NAD-CID000005892
Running Enrichment Score
Ranked List Metric
Rank in Ordered Dataset
D
GO_MF_MM_TRIGLYCERIDE_LIPASE_ACTIVITY
HUMANCYC_MM_TRIACYLGLYCEROL_DEGRADATION
LIT_MM_PINENT_ATGL_CM_DN
STITCH_MM_CHOLESTEROL-CID000005997
STITCH_MM_COENZYME_A-CID100000317
STITCH_MM_OLEIC_ACID-CID000445639
STITCH_MM_PALMITATE-CID100000985
Running Enrichment Score
Ranked List Metric
Rank in Ordered Dataset
E
LIT_MM_BOSCH_INTESTINAL-DETOXIFICATION-ENZYME_24H_DIFF
LIT_MM_BOUTER_IAT-MITOCHONDRIAL-PEROXISOMAL-FUNCTIONS_RSG_DB_DB_DIFF
LIT_MM_SCHLUTER_OXIDATIVE-STRESS_DIFF
STITCH_MM_LIPOXIN_A4-CID100003934
Running Enrichment Score
Ranked List Metric
Rank in Ordered Dataset
F
Vascular smooth muscle contraction
Signaling pathways regulating pluripotency of stem cells
Regulation of actin cytoskeleton
Rap1 signaling pathway
Purine metabolism
Proteoglycans in cancer
PI3K–Akt signaling pathway
Pathways in cancer
Pancreatic secretion
Oxytocin signaling pathway
NOD–like receptor signaling pathway
Neuroactive ligand–receptor interaction
MAPK signaling pathway
Longevity regulating pathway
Insulin secretion
p. adjust
1.00
0.75
0.50
0.25
0.00
Count
7
8
9
10
11
12
13
0.010 0.015 0.020 0.025 0.030
GeneRatio

**Figure 6. The underlying mechanisms in the favorable effects of SF1 on ATP production**

(A) Islets from 3 HFD-fed male mice were isolated, transfected with Ad-GFP-Vector/SF1 (MOI = 100) respectively and analyzed by RNA-Seq. Heatmap of the differentially expressed genes (DEGs) in Ad-GFP-Vector vs SF1 DIO islets. The red lines represent up-regulated genes while the green ones represent down-regulated genes.

(B) GO analysis for DEGs in the biological processes (top), cellular component (middle) and molecular function (bottom) categories. BP, biological processes; CC, cellular component; MF, molecular function.

(C) GSEA analysis of gene signatures associated with mitochondrial functions.

(D) GSEA analysis of gene signatures associated with lipolysis.

(E) GSEA analysis of gene signatures associated with detoxication.

(F) KEGG analysis based on transcriptome profiling of MIN6-Vector vs SF1.

is worth noting that SF1 restores GSIS by improving mitochondrial ATP production in beta cells upon PA treatment, as demonstrated by our *in vitro* experiments. Additionally, bioinformatic analysis based on RNA-seq showed that the potential mechanisms included OXPHOS, NADPH, lipolysis, and detoxication. Accordingly, SF1 induces GSIS by fostering mitochondrial ATP synthesis and regulating lipid metabolism which is protective to beta cells. Nevertheless, the underlying mechanisms remain to be further elucidated.

Our data reinforce the tempting concept that SF1 promises to delay beta-cell decompensation in defense against obesity-induced diabetes suggesting its potential role as a therapeutic target for T2DM treatment. Of particular importance, the encouraging observation that AAV-mediated SF1 overexpression specifically in beta cells exerts a favorable metabolic phenotype *in vivo* sheds light on its clinical therapeutic benefits. Apart from this, SF1 is an ideal target for drugs as an orphan NR, similar to PPARγ whose agonist is rosiglitazone.[25] A series of small molecular agonists targeting SF1 have been developed but are yet to be used *in vivo*, which are potential to be exploited therapeutically for T2DM.[26,27]

In addition, research on how SF1 increases and declines at different stages in the T2DM progress may also provide ideas for upregulating SF1 expression in beta cells as a therapeutic strategy. It has been reported that both the expression and activity of SF1 are significantly promoted upon hyperactivation of insulin signaling, which leads to nuclear localization of forkhead box transcription factor O1 (FOXO1) in the VMH as well as adrenocortical Y1 cells.[28,29] Given that hyperactivation of insulin signaling occurs within beta cells at the early stage of peripheral insulin resistance, it is reasonable to speculate that high expression of SF1 in beta cells was the response to hyperinsulinemia.[30] It was reported that beta cells per se could represent insulin resistance in the advanced stage of diabetes.[31,32] We speculate that the descending trend of SF1 in long-term DIO and *db/db* mice may be explained by blockage of the insulin signaling pathway due to beta-cell insulin resistance. However, how the expression of SF1 is induced by insulin requires more investigation, which is expected to provide an economical and practical way to trigger SF1 upregulation *in vivo*.

In conclusion, we have substantiated that SF1 positively regulates GSIS in pancreatic beta cells by boosting ATP production. Upregulation of SF1 in obesity contributes to beta-cell compensation, and beta-cell failure in obesity-induced diabetes may be due to its downregulation. Therefore, SF1 may be an attractive therapeutic target to preserve and restore insulin secretion in defense against obesity-related diabetes.

## Limitations of the study

There are some limitations in this study. We focused on males in the *in vitro* studies as well as the *in vivo* studies using AAV therapy, since the impact of SF1 on glucose intolerance upon DIO appeared to be more robust in males, which could be explained by the inherent insensitivity of females to obesity-induced insulin resistance, as reported previously.[33,34] However, whether sexual dimorphism exists in the response of islets per se to SF1 deletion needs to be further investigated.

## STAR★METHODS

Detailed methods are provided in the online version of this paper and include the following:

- KEY RESOURCES TABLE
- RESOURCE AVAILABILITY
  - Lead contact
  - Materials availability
  - Data and code availability

## SUPPLEMENTAL INFORMATION

Supplemental information can be found online at https://doi.org/10.1016/j.isci.2023.106451.

## ACKNOWLEDGMENTS

We thank Prof. Han Xiao (Nanjing Medical University), who is well-experienced in the pathogenesis of diabetes and beta-cell dysfunction and the members of the key laboratory of Human Functional Genomics in Jiangsu Province for their advice and helpful discussions. We also thank Prof. Hu Anbin (Sun Yat-sen University) who has long been engaged in islet transplantation, and the members of the organ transplant department of the first affiliated hospital, Sun Yat-sen University for their help with the collection of human pancreas specimens. We thank HOME for Researchers for providing a platform Figdraw (https://www.figdraw.com/static/index.html) for us to complete our graphical abstract.

This work was supported by the National Key Research and Development Program of China (no. 2018YFC1314100) awarded to L.Y.B.; National Natural Science Foundation of China awarded to L.Y.B. (no. 81870557), G.Y. (no. 82200876), L.L.H. (no. 81800716), G.H.Y. (82073050) and W.X.S. (no. 82100895), respectively; the Key Field Research and Development Program of Guangdong Province, China (no. 2019B020230001) awarded to L.Y.B.; the Science and Technology Program of Guangzhou, China (no. 202002020053) awarded to L.L.H.; the Basic and Applied Basic Research Foundation of Guangdong Province, China (no. 2020A1515010049) awarded to L.H.; and the Graduate Innovative Development Program (no. 19ykyjs08) awarded to G.Y.

## AUTHOR CONTRIBUTIONS

Conceptualization, L.Y.B. and G.Y.; Methodology, G.Y., L.L.H., G.H.Y., C.X.P., L.J., W.X.S., L.H., L.W.W., and Z.P.Y.; Validation, G.Y., L.L.H., C.Y.L., G.H.Y., and L.Y.B.; Formal Analysis, G.Y., L.L.H., and G.H.Y.; Resources, X.H.P., C.X.P., W.X.S., and L.H.; Investigation, G.Y., C.Y.L., M.J.J., and C.J.; Data Curation, L.Y.B., G.Y., and L.L.H.; Writing-Original Draft, G.Y. and L.Y.B.; Writing-Review & Editing, L.Y.B., X.H.P., G.Y., G.H.Y., L.L.H., and C.Y.L.; Visualization, G.Y.; Supervision, L.Y.B., X.H.P., and G.H.Y.; Project Administration, L.Y.B.; Funding Acquisition, L.Y.B., G.Y., G.H.Y., L.L.H., L.H., and W.X.S.

## DECLARATION OF INTERESTS

The authors declare no competing interests.

## INCLUSION AND DIVERSITY

We support inclusive, diverse, and equitable conduct of research.

Received: September 15, 2022
Revised: February 12, 2023
Accepted: March 15, 2023
Published: March 20, 2023

## REFERENCES

1. Hudish, L.I., Reusch, J.E., and Sussel, L. (2019). Beta Cell dysfunction during progression of metabolic syndrome to type 2 diabetes. J. Clin. Invest. *129*, 4001–4008. https://doi.org/10.1172/JCI129188.

2. Kahn, S.E. (2003). The relative contributions of insulin resistance and beta-cell dysfunction to the pathophysiology of Type 2 diabetes. Diabetologia *46*, 3–19. https://doi.org/10.1007/s00125-002-1009-0.

3. Ye, R., Gordillo, R., Shao, M., Onodera, T., Chen, Z., Chen, S., Lin, X., SoRelle, J.A., Li, X., Tang, M., et al. (2018). Intracellular lipid metabolism impairs beta cell compensation during diet-induced obesity. J. Clin. Invest. *128*, 1178–1189. https://doi.org/10.1172/JCI97702.

4. Huang, P., Chandra, V., and Rastinejad, F. (2010). Structural overview of the nuclear receptor superfamily: insights into physiology and therapeutics. Annu. Rev. Physiol. *72*, 247–272. https://doi.org/10.1146/annurev-physiol-021909-135917.

5. Parker, K.L., and Schimmer, B.P. (1997). Steroidogenic factor 1: a key determinant of endocrine development and function. Endocr. Rev. *18*, 361–377. https://doi.org/10.1210/edrv.18.3.0301.

6. Orozco-Solis, R., Aguilar-Arnal, L., Murakami, M., Peruquetti, R., Ramadori, G., Coppari, R., and Sassone-Corsi, P. (2016). The circadian clock in the ventromedial hypothalamus controls cyclic energy expenditure. Cell Metab. *23*, 467–478. https://doi.org/10.1016/j.cmet.2016.02.003.

7. Baba, T., Otake, H., Sato, T., Miyabayashi, K., Shishido, Y., Wang, C.Y., Shima, Y., Kimura, H., Yagi, M., Ishihara, Y., et al. (2014). Glycolytic genes are targets of the nuclear receptor Ad4BP/SF-1. Nat. Commun. *5*, 3634. https://doi.org/10.1038/ncomms4634.

8. Kim, K.W., Zhao, L., Donato, J., Jr., Kohno, D., Xu, Y., Elias, C.F., Lee, C., Parker, K.L., and Elmquist, J.K. (2011). Steroidogenic factor 1 directs programs regulating diet-induced thermogenesis and leptin action in the ventral medial hypothalamic nucleus. Proc. Natl. Acad. Sci. USA *108*, 10673–10678. https://doi.org/10.1073/pnas.1102364108.

9. Majdic, G., Young, M., Gomez-Sanchez, E., Anderson, P., Szczepaniak, L.S., Dobbins, R.L., McGarry, J.D., and Parker, K.L. (2002). Knockout mice lacking steroidogenic factor 1 are a novel genetic model of hypothalamic obesity. Endocrinology *143*, 607–614. https://doi.org/10.1210/endo.143.2.8652.

10. Liu, W., Liu, M., Fan, W., Nawata, H., and Yanase, T. (2006). The Gly146Ala variation in human SF-1 gene: its association with insulin resistance and type 2 diabetes in Chinese. Diabetes Res. Clin. Pract. *73*, 322–328. https://doi.org/10.1016/j.diabres.2006.02.007.

11. Mazilu, J.K., Powers, J.W., Lin, S., and McCabe, E.R.B. (2010). ff1b, the SF1 ortholog, is important for pancreatic islet cell development in zebrafish. Mol. Genet. Metab. *101*, 391–394. https://doi.org/10.1016/j.ymgme.2010.09.011.

12. Baetens, D., Stefan, Y., Ravazzola, M., Malaisse-Lagae, F., Coleman, D.L., and Orci, L. (1978). Alteration of islet cell populations in spontaneously diabetic mice. Diabetes *27*, 1–7. https://doi.org/10.2337/diab.27.1.1.

13. Nunes-Souza, V., César-Gomes, C.J., Da Fonseca, L.J.S., Guedes, G.D.S., Smaniotto, S., and Rabelo, L.A. (2016). Aging increases susceptibility to high fat diet-induced metabolic syndrome in C57BL/6 mice: improvement in glycemic and lipid profile after antioxidant therapy. Oxid. Med. Cell. Longev. *2016*, 1987960. https://doi.org/10.1155/2016/1987960.

14. Gannon, M., Kulkarni, R.N., Tse, H.M., and Mauvais-Jarvis, F. (2018). Sex differences underlying pancreatic islet biology and its dysfunction. Mol. Metab. *15*, 82–91. https://doi.org/10.1016/j.molmet.2018.05.017.

15. Nolan, C.J., and Prentki, M. (2008). The islet beta-cell: fuel responsive and vulnerable. Trends Endocrinol. Metab. *19*, 285–291. https://doi.org/10.1016/j.tem.2008.07.006.

16. Lu, H., Koshkin, V., Allister, E.M., Gyulkhandanyan, A.V., and Wheeler, M.B. (2010). Molecular and metabolic evidence for mitochondrial defects associated with beta-cell dysfunction in a mouse model of type 2 diabetes. Diabetes *59*, 448–459. https://doi.org/10.2337/db09-0129.

17. Kim, K.W., Sohn, J.W., Kohno, D., Xu, Y., Williams, K., and Elmquist, J.K. (2011). SF-1 in the ventral medial hypothalamic nucleus: a key regulator of homeostasis. Mol. Cell. Endocrinol. *336*, 219–223. https://doi.org/10.1016/j.mce.2010.11.019.

18. Kinyua, A.W., Yang, D.J., Chang, I., and Kim, K.W. (2016). Steroidogenic factor 1 in the ventromedial nucleus of the hypothalamus regulates age-dependent obesity. PLoS One *11*, e0162352. https://doi.org/10.1371/journal.pone.0162352.

19. Martin Vázquez, E., Cobo-Vuilleumier, N., Araujo Legido, R., Marín-Cañas, S., Nola, E., Dorronsoro, A., López Bermudo, L., Crespo, A., Romero-Zerbo, S.Y., García-Fernández, M., et al. (2022). NR5A2/LRH-1 regulates the PTGS2-PGE(2)-PTGER1 pathway contributing to pancreatic islet survival and function. iScience *25*, 104345. https://doi.org/10.1016/j.isci.2022.104345.

20. Detimary, P., Dejonghe, S., Ling, Z., Pipeleers, D., Schuit, F., and Henquin, J.C. (1998). The changes in adenine nucleotides measured in glucose-stimulated rodent islets occur in beta cells but not in alpha cells and are also observed in human islets. J. Biol. Chem. *273*, 33905–33908. https://doi.org/10.1074/jbc.273.51.33905.

21. Prentki, M., Corkey, B.E., and Madiraju, S.R.M. (2020). Lipid-associated metabolic signalling networks in pancreatic beta cell function. Diabetologia *63*, 10–20. https://doi.org/10.1007/s00125-019-04976-w.

22. Supale, S., Li, N., Brun, T., and Maechler, P. (2012). Mitochondrial dysfunction in pancreatic beta cells. Trends Endocrinol. Metab. *23*, 477–487. https://doi.org/10.1016/j.tem.2012.06.002.

23. Mugabo, Y., Zhao, S., Lamontagne, J., Al-Mass, A., Peyot, M.L., Corkey, B.E., Joly, E., Madiraju, S.R.M., and Prentki, M. (2017). Metabolic fate of glucose and candidate signaling and excess-fuel detoxification pathways in pancreatic beta-cells. J. Biol. Chem. *292*, 7407–7422. https://doi.org/10.1074/jbc.M116.763060.

24. van Raalte, D.H., and Verchere, C.B. (2017). Improving glycaemic control in type 2 diabetes: stimulate insulin secretion or provide beta-cell rest? Diabetes Obes. Metab. *19*, 1205–1213. https://doi.org/10.1111/dom.12935.

25. Wang, S., Dougherty, E.J., and Danner, R.L. (2016). PPARgamma signaling and emerging opportunities for improved therapeutics. Pharmacol. Res. *111*, 76–85. https://doi.org/10.1016/j.phrs.2016.02.028.

26. Whitby, R.J., Dixon, S., Maloney, P.R., Delerive, P., Goodwin, B.J., Parks, D.J., and Willson, T.M. (2006). Identification of small molecule agonists of the orphan nuclear receptors liver receptor homolog-1 and steroidogenic factor-1. J. Med. Chem. *49*, 6652–6655. https://doi.org/10.1021/jm060990k.

27. Whitby, R.J., Stec, J., Blind, R.D., Dixon, S., Leesnitzer, L.M., Orband-Miller, L.A., Williams, S.P., Willson, T.M., Xu, R., Zuercher,

W.J., et al. (2011). Small molecule agonists of the orphan nuclear receptors steroidogenic factor-1 (SF-1, NR5A1) and liver receptor homologue-1 (LRH-1, NR5A2). J. Med. Chem. *54*, 2266–2281. https://doi.org/10.1021/jm1014296.

28. Kim, K.W., Donato, J., Jr., Berglund, E.D., Choi, Y.H., Kohno, D., Elias, C.F., Depinho, R.A., and Elmquist, J.K. (2012). FOXO1 in the ventromedial hypothalamus regulates energy balance. J. Clin. Invest. *122*, 2578–2589. https://doi.org/10.1172/JCI62848.

29. Kinyua, A.W., Doan, K.V., Yang, D.J., Huynh, M.K.Q., Choi, Y.H., Shin, D.M., and Kim, K.W. (2018). Insulin regulates adrenal steroidogenesis by stabilizing SF-1 activity. Sci. Rep. *8*, 5025. https://doi.org/10.1038/s41598-018-23298-2.

30. Kubota, T., Kubota, N., and Kadowaki, T. (2017). Imbalanced insulin actions in obesity and type 2 diabetes: key mouse models of insulin signaling pathway. Cell Metab. *25*, 797–810. https://doi.org/10.1016/j.cmet.2017.03.004.

31. Zheng, S., Chen, N., Kang, X., Hu, Y., and Shi, S. (2022). Irisin alleviates FFA induced beta-cell insulin resistance and inflammatory response through activating PI3K/AKT/FOXO1 signaling pathway. Endocrine *75*, 740–751. https://doi.org/10.1007/s12020-021-02875-y.

32. Liu, S., Li, X., Yang, J., Zhu, R., Fan, Z., Xu, X., Feng, W., Cui, J., Sun, J., and Liu, M. (2019). Misfolded proinsulin impairs processing of precursor of insulin receptor and insulin signaling in beta cells. FASEB J *33*, 11338–11348. https://doi.org/10.1096/fj.201900442R.

33. Casimiro, I., Stull, N.D., Tersey, S.A., and Mirmira, R.G. (2021). Phenotypic sexual dimorphism in response to dietary fat manipulation in C57BL/6J mice. J. Diabetes Complications *35*, 107795. https://doi.org/10.1016/j.jdiacomp.2020.107795.

34. Mauvais-Jarvis, F., Arnold, A.P., and Reue, K. (2017). A guide for the design of pre-clinical studies on sex differences in metabolism. Cell Metab. *25*, 1216–1230. https://doi.org/10.1016/j.cmet.2017.04.033.

35. Yu, G., Wang, L.G., Han, Y., and He, Q.Y. (2012). clusterProfiler: an R package for comparing biological themes among gene clusters. OMICS *16*, 284–287. https://doi.org/10.1089/omi.2011.0118.

36. Xiong, L., Chen, L., Wu, L., He, W., Chen, D., Peng, Z., Li, J., Zhu, X., Su, L., Li, Y., et al. (2022). Lipotoxicity-induced circGlis3 impairs beta cell function and is transmitted by exosomes to promote islet endothelial cell dysfunction. Diabetologia *65*, 188–205. https://doi.org/10.1007/s00125-021-05591-4.

37. Guo, Y., Li, H., Guan, H., Ke, W., Liang, W., Xiao, H., and Li, Y. (2019). Dermatopontin inhibits papillary thyroid cancer cell proliferation through MYC repression. Mol. Cell. Endocrinol. *480*, 122–132. https://doi.org/10.1016/j.mce.2018.10.021.

38. Guo, Y., Li, H., Chen, X., Yang, H., Guan, H., He, X., Chen, Y., Pokharel, S., Xiao, H., and Li, Y. (2020). Novel roles of chloroquine and hydroxychloroquine in graves' orbitopathy therapy by targeting orbital fibroblasts. J. Clin. Endocrinol. Metab. *105*, 1906–1917. https://doi.org/10.1210/clinem/dgaa161.

39. Zhao, C., Qiao, C., Tang, R.H., Jiang, J., Li, J., Martin, C.B., Bulaklak, K., Li, J., Wang, D.W., and Xiao, X. (2015). Overcoming insulin insufficiency by forced follistatin expression in beta-cells of db/db mice. Mol. Ther. *23*, 866–874. https://doi.org/10.1038/mt.2015.29.

40. Chen, X., He, X., Guo, Y., Liu, L., Li, H., Tan, J., Feng, W., Guan, H., Cao, X., Xiao, H., and Li, Y. (2021). Glucose-dependent insulinotropic polypeptide modifies adipose plasticity and promotes beige adipogenesis of human omental adipose-derived stem cells. FASEB J. *35*, e21534. https://doi.org/10.1096/fj.201903253R.

## STAR★METHODS

### KEY RESOURCES TABLE

| REAGENT or RESOURCE | SOURCE | IDENTIFIER |
|---|---|---|
| **Antibodies** | | |
| Mouse monoclonal anti-SF1 antibody (A-1) | Santa Cruz Biotechnology | Cat# sc-393592; Lot# H3121 |
| SF1 (A-1) blocking peptide | Santa Cruz Biotechnology | Cat# sc-393592 P Lot# 10717 |
| Mouse monoclonal anti-Glucagon antibody (K79bB10) | Abcam | Cat# ab10988; RRID: AB_297642; Lot# GR3208749-20 |
| Mouse monoclonal anti-Insulin (2D11-H5) | Santa Cruz Biotechnology | Cat# sc-8033; RRID: AB_627285 Lot# G3120 |
| Rabbit monoclonal anti-β-Actin (13E5) | Cell Signaling Technology | Cat# 4970; RRID: AB_2223172 Lot# 11 |
| Rabbit monoclonal anti-Flag (D6W5B) | Cell Signaling Technology | Cat# 14793; RRID:AB_2572291 Lot# 5 |
| Goat anti-Rabbit IgG H&L (HRP) | Abcam | Cat# ab6721; RRID: AB_955447 Lot# GR3242092-2 |
| Goat anti-Mouse IgG H&L (HRP) | Abcam | Cat# ab205719; RRID: AB_2755049 Lot# GR3405228-11 |
| **Bacterial and virus strains** | | |
| AAV8-Ins1-SF1 | Vigene Biosciences | N/A |
| AAV8-Ins1-Vector | Vigene Biosciences | N/A |
| Ad-GFP-SF1 | Vigene Biosciences | N/A |
| Ad-GFP-Vector | Vigene Biosciences | N/A |
| **Biological samples** | | |
| Human pancreas (listed Table S1) | The First Affiliated Hospital of Sun Yat-sen University | N/A |
| Human testis (listed Table S1) | The First Affiliated Hospital of Sun Yat-sen University | N/A |
| Mouse pancreas | The First Affiliated Hospital of Sun Yat-sen University | N/A |
| Mouse testis | The First Affiliated Hospital of Sun Yat-sen University | N/A |
| **Chemicals, peptides, and recombinant proteins** | | |
| 4% Paraformaldehyde (PFA) | Biosharp | Cat# BL539A |
| Triton X-100 | Solarbio | Cat# T8200 |
| Opal 520 Reagent | Asbio | Cat# ASOP520 |
| Opal 570 Reagent | Asbio | Cat# ASOP570 |
| ProLong™ Gold (DAPI) | Invitrogen | Cat# P36935 |
| Tamoxifen | Sigma-Aldrich | Cat# T5648 |
| Corn oil | Solarbio | Cat# C7030 |

(*Continued on next page*)

*Continued*

| REAGENT or RESOURCE | SOURCE | IDENTIFIER |
|---|---|---|
| Avertin | Sigma-Aldrich | Cat# T48402 |
| Collagenase P | Sigma-Aldrich | Cat# 11213857001 |
| Krebs-Ringer bicarbonate HEPES buffer (KRBH) | LEAGENE | Cat# CZ0103 |
| Hank's balanced salt solution (HBSS) | Hyclone | Cat# SH30030.02 |
| Palmitate Acid (PA) | Sigma-Aldrich | Cat# 489662 |
| Bovine serum albumin (BSA) | Bovogen | Cat# BSAS |
| 8-Br-cAMP | Sigma-Aldrich | Cat# B7880 |
| X-Rhod-1, AM | Invitrogen | Cat# X14210 |
| Fetal bovine serum (FBS) | Gibco | Cat# 10270106 |
| Dulbecco's modified eagle medium (DMEM) | Gibco | Cat# C11995500BT |
| RPMI 1640 | Gibco | Cat# C11875500BT |
| Beta-mercaptoethanol | Gibco | Cat# 21985023 |
| Antibiotics (P/S) | Sorlabio | Cat# P1400 |
| TRIzol™ Reagent | Invitrogen | Cat# 15596018 |
| Seahorse XF DMEM medium | Agilent | Cat# 103575-100 |
| **Critical commercial assays** | | |
| Mouse insulin ELISA kit | Mercodia | Cat# 10-1247-01 |
| RNAscope® 2.5 HD detection kit | ACD | Cat# 322360 |
| RNAscope® multiplex fluorescent reagent kit | ACD | Cat# 323100 |
| MycoAlert PLUS mycoplasma detection kit | Lonza | Cat# LT07-710 |
| Seahorse XF cell mito stress test kit | Agilent | Cat# 103015-100 |
| Pierce™ BCA protein assay kit | Thermo Fisher Scientific | Cat# 23227 |
| QIAamp DNA micro kit | Qiagen | Cat# 56304 |
| ATP determination kit | Sigma-Aldrich | Cat# MAK190 |
| **Deposited data** | | |
| RNA-seq data of islets from male HFD-fed mice transfected with Ad-GFP-Vector/SF1 | This paper, NCBI SRA | SRA: PRJNA926099 |
| RNA-seq data of MIN6-Vector/SF1 | This paper, NCBI SRA | SRA: PRJNA932995 |
| **Experimental models: Cell lines** | | |
| MIN6 | AddexBio | Cat# C0018008/403; RRID:CVCL_0431 |
| 293FT | National Infrastructure of Cell Line Recource (NICR) of China | Cat# 1101HUM-PUMC000364 |
| **Experimental models: Organisms/strains** | | |
| Mouse: C57BL/6J | GemPharmatech Co., Ltd. | Cat# N000013 |
| Mouse: C57BL/KsJ | GemPharmatech Co., Ltd. | Cat# N000214 |
| Mouse: *ob/ob* mice: B6/JGpt-Lepem1Cd25/Gpt | GemPharmatech Co., Ltd. | Cat# T001461 |
| Mouse: *db/db* mice: BKS-Leprem2Cd479/Gpt | GemPharmatech Co., Ltd. | Cat# T002407 |
| Mouse: Pdx1-CreER: Tg (Pdx1-cre/Esr1*)#Dam | The Jackson Laboratory | JAX: 024968 |
| Mouse: $SF1^{fl/fl}$: C57BL/6J: B6/JNju-Nr5a1em1Cflox/Gpt | GemPharmatech Co., Ltd. | Cat# T009872 |
| **Oligonucleotides** | | |
| RNAscope® probe-Mm-Nr5a1 | ACD | Cat# 445731 |

(*Continued on next page*)

*Continued*

| REAGENT or RESOURCE | SOURCE | IDENTIFIER |
|---|---|---|
| RNAscope® probe-Hs-NR5A1 | ACD | Cat# 553151-1 |
| RNAscope® positive control probe-Mm-Ppib | ACD | Cat# 313911 |
| RNAscope® positive control probe-Hs-PPIB | ACD | Cat# 313901 |
| RNAscope® negative control probe-DapB | ACD | Cat# 310043 |
| Primers for PCR, see Table S2 | This Paper | N/A |
| **Recombinant DNA** | | |
| pSin-SF1-Flag | This Paper | N/A |
| pSin-Vector | This Paper | N/A |
| **Software and algorithms** | | |
| ImageJ | ImageJ | https://imagej.nih.gov/ij/ |
| Graphpad Prism | Graphpad | https://www.graphpad.com/ |
| Adobe Photoshop | Adobe | https://www.adobe.com/es/ |
| SPSS 26.0 | IBM | https://www.ibm.com/uk-en/analytics/spss-statistics-software |
| clusterProfiler v. 4.0.5 | Yu, G., et al.[35] | http://bioconductor.org/packages/release/bioc/html/clusterProfiler.html |
| Figdraw | HOME for Researchers | https://www.figdraw.com/static/index.html |
| **Other** | | |
| Rodent diet with 60 kcal% fat | Research Diets Inc. | Cat #D12492 |
| Accu-Chek active glucometer | Roche Diagnostics GmbH | N/A |
| Lionheart FX automated live cell imager | BioTex | N/A |
| Seahorse XF96 analyzer | Agilent | N/A |

## RESOURCE AVAILABILITY

### Lead contact

Further information and requests for resources and reagents should be directed to and will be fulfilled by the lead contact, Yanbing Li (liyb@mail.sysu.edu.cn).

### Materials availability

This study did not generate any new unique reagents.

### Data and code availability

- RNA-seq data have been deposited at Sequence Read Archive and are publicly available as of the date of publication. Accession numbers are listed in the key resources table.
- This paper does not include the original code.
- Any additional information required to reanalyze the data in this paper is available from the lead contact upon request.

## EXPERIMENTAL MODEL AND SUBJECT DETAILS

### Mice

C57BL/6J mice, C57BL/KsJ, *ob/ob* and *db/db* mice were purchased from GemPharmatech Company. We fed 8-week-old C57BL/6J male mice with a HFD regimen (60% energy from fat, Research Diets, Inc.) to generate a diet-induced obesity (DIO) model, while the control counterparts were subjected to a Chow diet (18% energy from fat).

The strains used for CKO mouse generation were all on the C57BL/6J background. Floxed SF1 ($SF1^{fl/fl}$) mice were established using CRISPR/Cas9. The $SF1^{fl/fl}$ mouse line was crossed with the Pdx1-CreER mouse line

(Jackson Laboratories), which harbors a tamoxifen (TAM)-inducible Cre recombinase/estrogen receptor fusion protein under the transcriptional control of the Pdx1 promoter. These mice were injected daily with TAM (100 mg/kg) for 10 days to generate $\beta SF1^{+/+}$, $\beta SF1^{+/-}$ and $\beta SF1^{-/-}$ mice. Both females (20 weeks old) and males (12 weeks old) of different genotypes were subjected to a Chow diet or a HFD regimen, before subsequent experiments.[13]

Mice were housed in ventilated cages on a 12-h light:12-h dark cycle at constant temperature (22–24°C) and given food and water adlibitum unless otherwise stated. At termination of metabolic studies, mice were euthanized and organs (islets, pancreas, liver, adipose and hypothalamus) were extracted for subsequent analysis.

### Primary mouse islets

Pancreatic islets were isolated from mice at the indicated age in the manuscript. Following anesthetization using Avertin (Sigma-Aldrich), the pancreas was perfused with about 3 ml Hank's balanced salt solution (HBSS, Hyclone) containing 1.5 mg/mL collagenase P (Sigma-Aldrich) via the pancreatic duct. Digested in a water bath at 37°C for apropos time, the pancreas was then vortexed for 30 sec and added 25 mL HBSS containing 10% (vol/vol) fetal bovine serum (FBS, Gibco). After being washed 2 times with FBS-free HBSS, islets were manually picked by pipette under a stereomicroscope and incubated in RPMI 1640 (Gibco) containing 10% FBS at 37°C before experiments.

### Cell lines

MIN6 cells (passages 8–16, AddexBio) were grown in Dulbeccos modified Eagle's medium (DMEM) supplemented with 15% FBS, 100 units/ml penicillin plus 10 μg/ml streptomycin (P1400, Solarbio), and 50 μM beta-mercaptoethanol (21985023, Gibco) and maintained in a humidified incubator with 95% air and 5% $CO_2$ at 37°C, as described previously.[36] For MIN6-SF1/Vector stable cell lines, a pSin-SF1-Flag Vector and the control Vector were transfected into 293FT cell line (National Infrastructure of Cell Line Resource, NICR) to produce virus suspension. Detailed steps were as previously described.[37] All cells were validated to be mycoplasma-free using the MycoAlert PLUS Mycoplasma Detection Kit (Lonza).

### Study approval

All animal experiments followed the rules and guidelines of the Animal Care and Use Committee of the First Affiliated Hospital of Sun Yat-sen University. The study protocol was approved by the Animal Care and Use Committee of the First Affiliated Hospital of Sun Yat-sen University. Human pancreas and testis specimens were obtained with the approval of the institutional research ethics committee in the First Affiliated Hospital of Sun Yat-sen University, listed in Table S1. Written informed consent was obtained from each patient.

## METHOD DETAILS

### Metabolic studies

Intraperitoneal (i.p.) GTTs, glucose-stimulated insulin secretion (GSIS) tests and fasting-refeeding tests were performed on 15 h overnight-fasted mice, and i.p. ITTs on 5 h-fasted mice (17 h specially for the *db/db* mice). For fasting and refeeding tests, blood glucose levels were measured in fasted mice and 5 h after refeeding. Blood glucose and plasma insulin were assessed at the indicated times using an Accu-Chek Active glucometer (Roche Diagnostics GmbH) and insulin ELISA kit (Mercodia), respectively.

### Tissue collection and histological analysis

Mice were euthanized and organs (islets, pancreas, liver, adipose and hypothalamus) of each animal were dissected, and fixed in 4% (wt/vol.) paraformaldehyde for 24 h at 4°C and embedded in paraffin for further histological analysis.

### Immunofluorescence (IF) incorporating tyramide signal amplification

Sections for IF were incubated overnight at 4°C with mouse anti-Insulin antibody (1:200, Santa Cruz Biotechnology). The samples were then incubated with the corresponding horseradish peroxidase (HRP)-conjugated second antibody, goat anti-mouse (1:400, Abcam) for 30 min at room temperature (RT) before being incubated with the appropriate Opal fluorophore-conjugated tyramide signal amplification (TSA) (ASOP520, Asbio) for 10 min at RT. Following HRP blocking at 40°C, slides were subjected to

microwave-induced epitope retrieval for 25 min in 10 mM citrate buffer (pH 6.0), before being stained by another primary antibody mouse anti-SF1 (1:50, Santa Cruz Biotechnology), followed by repeating the steps described. The slides were rinsed with washing buffer after each step. The slides were mounted using ProLong Gold with 4′,6-diamidino-2-phenylindole (DAPI) (Thermo Fisher Scientific) and then imaged with a microscope (FV3000, Olympus).

### Hematoxylin-eosin (HE) staining and islet morphometry

Pancreas sections were stained with HE to assess morphology, according to a standard method.[37] The HE-stained sections were photographed using light microscopy microscope (IX71, Olympus). Pancreatic sections immunoprobed for mouse anti-Insulin antibody (1:200, Santa Cruz Biotechnology), mouse anti-Glucagon antibody (1:200, Abcam) and a nuclear stain (DAPI) were scanned with a microscope (IX71, Olympus).

### *In situ* hybridization (RNAscope)

Human pancreas/testis slides were stained for SF1 mRNA according to the instructions of the RNAscope multiplex fluorescent reagent kit (323100, ACD) and photographed using an confocal microscope (LSM800, Zeiss). Mouse pancreas/testis slides were stained for SF1 mRNA using the RNAscope 2.5 HD Detection Kit (322360, ACD), and photographed using a microscope (IX71, Olympus). RNA probes targeting SF1 (ACD445731 for mouse; ACD553151-1 for human), positive control probes targeting Hs-PPIB (313901, ACD), Mm-Ppib (313911, ACD) and negative control probe targeting DapB (310043, ACD) were respectively applied to the samples. All steps followed the instructions of the kits.

### DNA extraction and polymerase chain reaction (PCR)

Genomic DNA of islets from $\beta SF1^{+/+}$ and $\beta SF1^{-/-}$ mice was extracted using a Kit (56304, Qiagen) one week after TAM injection and analyzed by PCR production on 1% agarose gel. PCR was conducted using specific primers which are respectively targeted to the upwards and downward of the floxed-SF1 locus (see Table S2).

### Immunoblotting

Immunoblotting was conducted according to a standard method, as described previously.[38] The following primary antibodies were used for immunoblotting: rabbit anti-Flag antibody (1:1000, Cell Signaling Technology), rabbit anti-β-actin antibody (1:1000, Cell Signaling Technology), and mouse anti-SF1 antibody (1:500, Santa Cruz Biotechnology).

### Adeno-associated virus mediated steroidogenic factor 1 overexpression *in vivo*

As previously reported, intraperitoneal injection of an AAV8 Vector driven by an Ins1 promoter rendered strong and highly specific gene expression in beta cells.[39] AAV8 with Ins1 promoter driving SF1 expression (AAV8-Ins1-SF1) and the control AAV8-Ins1-Vector were constructed by Vigene Biosciences, as previously described.[13] AAV8 was used described previously.[13]

### Adenoviral (Ad) infection of islets

An adenovirus encoding mouse SF1 (Ad-GFP-SF1) and the control Ad-GFP-Vector were produced by Vigene Biosciences. Ad-GFP-SF1/Vector were administered to the cultured islets at multiplicity of infection (MOI) of 100 for 48 h before measurements.

### Preparation of palmitate (Palmitate Acid) BSA stock solution

A stock solution of PA (489662, Sigma Aldrich) was prepared as previously described.[13] Briefly, 40 mM PA in 0.15 mM sodium chloride was incubated at 70°C for 60 min. Simultaneously, 10% (w/v) fatty acid-free BSA (BSAS 1.0, BovoStar) was incubated at 37°C for 60 min, in 0.15 mM sodium chloride and filter sterilized. The PA and BSA solutions were mixed 1:1, vortex and incubated in shaking heating block at 55°C overnight. The stock solutions (20 mM) were supplemented into the cultivation media at required final concentrations.

### Insulin secretion tests *ex vivo*

Islets kept in PA (0.4 mM) were incubated in Krebs-Ringer bicarbonate HEPES buffer (KRBH, containing 0.2% BSA, 20 mM HEPES, pH 7.2, 114 mM NaCl, 4.7 mM KCl, 1.2 mM $KH_2PO_4$, 1.16 mM $MgSO_4$ and

2.5 mM $CaCl_2$) for 30 min at 37°C. The buffer was replaced with that containing the indicated concentrations of glucose or 30 mM KCl (in 3 mM glucose). Supernatant without cells were collected for insulin measurement using a mouse insulin ELISA kit (10-1247-01, Mercodia).

### ATP measurements

To determine intracellular ATP levels, 10 islets/well with comparable sizes were incubated in the KRBH buffer without glucose 37°C for 30 min. The buffer was replaced with that containing 3.3 mM or 16.7 mM glucose respectively for 10 min before being lyzed to release ATP on ice which was then measured using the ATP Determination kit (MAK190-1KT, Sigma-Aldrich) and normalized with the islet numbers.

### Mitochondrial oxygen consumption rate

The OCR was measured in isolated islets or MIN6 cells using the Agilent Seahorse XF96 Analyzer and Seahorse XF Cell Mito Stress Test Kit (103015-100, Agilent), as previously described.[40] MIN6-Vector/SF1 were placed in 96-well plates at a density of 1.5 × 10^4/pole. Isolated islets (25 islets/well) were adhered in 96-well plates using Cell-Tak™ (354240, Corning). After MIN6 and the isolated islets were pre-treated as indicated in figure legends, the culture media were changed into DMEM (5.6 mM glucose) supplied with 15% FBS overnight before experiments. In detection buffer containing glutamine (2 mM) and pyruvate (2 mM for MIN6, 10 mM for islets) without glucose or $CO_2$, MIN6 or islets were then stimulated consecutive with glucose (28 mM for MIN6, 20 mM for islets), oligomycin (2 μM), carbonyl cyanide 4-(trifluoromethoxy) phenylhydrazone (FCCP, 1 μM) and 1 μM/1 μM rotenone/ antimycin (RA). OCR were calculated by seahorse XF analyzer and normalized to total protein content. Protein was extracted with sample buffer, and total protein content was determined by Pierce BCA kit (23227, Thermo Scientific).

### Measurement of intracellular $Ca^{2+}$ concentration

MIN6-Vector/SF1 were seeded in 48-well plates at a density of 2.5 × 10^4/pole with DMEM (25 mM glucose) supplied with 15% FBS at 37°C. Before calcium influx detection, MIN6-Vector/SF1 were kept in PA (0.4 mM) and cultivated in DMEM (5.6 mM glucose) supplied with 15% FBS overnight. After being loaded with 5 μM X-Rhod-1 AM (X14210, Thermo Scientific) in KRBH without glucose at 37°C for 30min, MIN6-Vector/SF1 were rinsed and de-esterified in KRBH without glucose. Stimulated with 30 mM KCl, fluorescent images were captured for 3 min at 1-sone-sec intervals by a Lionheart FX Automated Live Cell Imager (BioTex), as previously described.[40] Fluorescent intensity was recorded and normalized to average the base-line values (recorded for 30 sec before stimulation) to facilitate comparisons between responses in different cells.

### RNA sequencing and functional enrichment analysis

Total RNA extracted from Ad-SF1/Vector HFD murine islets and MIN6-Vector/SF1 with TRIzol reagent (15596018, Invitrogen) was evaluated using Agilent 2100 BioAnalyzer (Agilent Technologies) and Qubit Fluorometer (Invitrogen). Total RNA samples with RNA integrity number (RIN) > 7.0 and 28S:18S ratio >1.8 were used in the subsequent generation and sequencing of RNA-seq libraries by CapitalBio Technology.

GO analysis, GSEA and KEGG was performed using the R package "clusterProfiler".[35] Gene sets with adjusted $p < 0.05$ were defined as statistically significant.

## QUANTIFICATION AND STATISTICAL ANALYSIS

The data are presented as the mean ± standard error of the mean (SEM) and were analyzed by applying independent-samples t tests, one-way analysis of variance (least significant difference) or nonparametric test (Mann-Whitney tests) using SPSS 26.0 software (SPSS Inc.). Statistical significance required $p < 0.05$.